A LOW NOISE OSCILLATOR

BY EUGENE A. JANNING, JR.

JUNE, 1967

TABLE OF CONTENTS

INTRODUCTION

Most existing HF (2 to 30 MHz) radio receivers are grossly inadequate for many intended applications. This is primarily due to the increasingly overcrowded conditions of this frequency spectrum since many long-range radio communications links presently use this spectrum because of its desirable wave propagation characteristics. The situation is not likely to improve until UHF satellite communications links alleviate the problem.

Typical HF Communications Receivers have a useable sensitivity of -120 dBm (10^{-15} watts, 3 kHz bandwidth). Transmitters in this spectrum operating in the kilowatt region are commonplace, and it is not unusual to find signals on a receiving antenna from a local transmitter on the order of +20 dBm. Thus the receiver must be capable of processing extremely weak signals in the presence of very strong (140 dB greater) interfering signals occupying adjacent channels. For fixed-station or land-based operations, the problem may be alleviated somewhat by locating the receiving antennas at some distance from the transmitting antennas. For mobile operations, however, such as are encountered on aircraft or seagoing vessels, separation of the antennas is not generally practicable.

Although HF receivers have been under constant development for more than three decades, only recently have any significant strides been made toward improving dynamic range to the ultimate goal of 140 dB. (Typical HF receivers exhibit a dynamic range of 80-90 dB for adjacent channel interfering signals.) The dynamic

range referred to here could be more accurately described as de-sensitization, that is, the receiver is rendered insensitive to a weak desired signal by the presence of a strong interfering signal. De-sensitization may be caused by several mechanisms:

1) Saturation or non-linearity of the active circuitry, causing a loss in gain to the desired signal.

2) Heterodyning of spurious signals from the receiver frequency conversions (or other internal signals) into the receiver passband.

3) Heterodyning of noise from the receiver local oscillators into the receiver passband, causing an increase in noise in the desired channel.

Until quite recently, the limitation of receiver dynamic range has been due to saturation of the active circuitry. Parametric amplifiers, however, have eliminated this problem and it is not difficult to provide a parametric amplifier with a linear range of 140 dB over the HF band. Spurious signals may be eliminated by rigorous design and adequate shielding. Thus, the dynamic range of HF receivers is presently limited by noise on the receiver local oscillators which is heterodyned into the receiver passband by strong interfering signals.

OBJECTIVE

The primary objective of this thesis is to develop an analytical design procedure to enable the optimum design of a low noise oscillator for use as a pump source for a parametric amplifier used in a wide dynamic range HF receiver. The desired specification is:

1) Frequency Range; continuously tunable from 94.7 MHz to 122.7 MHz.

2) Power Output; 0 dBm nominal.

3) Output Noise Spectrum; extraneous noise power output in a 1 Hz bandwidth shall be a minimum of 145 dB below the desired output at all frequencies removed from the desired output by greater than 50 kHz (-110 dB for 3 kHz bandwidth).

It is desirable that the oscillator be all solid state and contain no moving parts (all tuning accomplished electronically). The initial design may not necessarily be temperature compensated but must be capable of compensation over the range from -55°C to +85°C. The frequency stability of the oscillator is not critical since it is intended for use with a frequency synthesizer. Other criteria such as size, weight, power consumption, etc., are of secondary importance.

A major thesis objective is to arrive at a design analysis technique which will reliably predict the noise power spectral density of an electronically-tuned oscillator and allow the synthesis of an optimum design.

A secondary objective is the development of a suitable measurement technique which will provide accurate, repeatable measurement of the oscillator noise power spectrum.

I. OSCILLATOR NOISE SPECTRUM

A. Theoretical Characterization of Oscillator Spectra

The output voltage (or current) from an oscillator may be described[1] mathematically by

$$v(t) = E(t) \cos\left[\omega_o t + \phi(t)\right] \tag{1}$$

where $E(t)$ and $\phi(t)$ are narrow-band (with respect to ω_o) stationary random processes and ω_o is a constant (carrier frequency). $E(t)$ is the amplitude or envelope function describing amplitude variations from the mean value, $\overline{E}$. $\phi(t)$ describes variations of phase from the ideal. ω_o and the time origin are chosen such that the mean value of $\phi(t)$ is zero.

Thus the oscillator output may be characterized by a single spectral line which is both amplitude and frequency modulated by stationary random functions of time. The process described by (1) may be assumed to be a narrow-band Gaussian random process. Under this assumption, it has been shown[2] that the random variable E_t, which defines the possible values of $E(t)$, possesses a Rayleigh probability density function. Also the random variable ϕ_t, which defines the possible values of $\phi(t)$, possesses a uniform probability density function over the interval $0 \leq \phi_t \leq 2\pi$. E_t and ϕ_t are statistically independent. However the envelope and phase random processes, $E(t)$ and $\phi(t)$, are not statistically independent.

The instantaneous angular frequency, $\omega_i(t)$, is

$$\omega_i(t) = \frac{d}{dt}\left[\omega_o t + \phi(t)\right] = \omega_o + \dot{\phi}(t) \qquad (2)$$

where $\dot{\phi}(t) = \frac{d}{dt}\phi(t)$. From (1) and (2) it is apparent that $\phi(t)$ is the instantaneous oscillator phase angle, and $\dot{\phi}(t)$ the instantaneous frequency departure from ω_o.

It is convenient to define several characterizations of oscillator performance or oscillator spectral densities.

1) The complete RF spectrum of the oscillator; $S_{RF}(\omega)$
2) The spectral density of $E(t)$; $S_{AM}(\omega)$
3) The spectral density of $\phi(t)$; $S_{\phi}(\omega)$
4) The spectral density of $\dot{\phi}(t)$; $S_{\dot{\phi}}(\omega)$

For purposes of the present discussion the amplitude spectral density, $S_{AM}(\omega)$, will be ignored since for the intended application it is of negligible significance compared to the phase or frequency perturbations. With this assumption and also assuming low modulation indices, the RF power spectral density, $S_{RF}(\omega)$, is identical (with a scale factor) to the phase spectral density, $S_{\phi}(\omega)$, because only first-order sidebands are of any consequence. ω_m is the modulation, or offset, frequency associated with the noise-like variations of $\phi(t)$.

The spectral density of a random signal may be defined as the Fourier transform of its autocorrelation function[3]. Thus

$$\left[S_{\phi}(\omega) = \int_{-\infty}^{+\infty} R_{\phi}(\tau)\, \epsilon^{-j\omega\tau}\, d\tau \right] \tag{3}$$

where $R_{\phi}(\tau)$ is the autocorrelation of the phase and is defined as

$$R_{\phi}(\tau) = \overline{\phi(t) \cdot \phi(t-\tau)} \tag{4}$$

The bar signifies statistical average. The inverse Transform of (3) is

$$R_{\phi}(\tau) = \frac{1}{2\pi} \int_{-\infty}^{+\infty} S_{\phi}(\omega)\, \epsilon^{j\omega\tau}\, d\omega \tag{5}$$

For $\tau = 0$, (4) and (5) reduce to

$$R_{\phi}(0) = \overline{\phi^2(t)} \tag{6}$$

$$R_{\phi}(0) = \frac{1}{2\pi} \int_{-\infty}^{+\infty} S_{\phi}(\omega)\, d\omega \tag{7}$$

Combining (6) and (7), we obtain

$$\overline{\phi^2(t)} = \frac{1}{2\pi} \int_{-\infty}^{+\infty} S_{\phi}(\omega)\, d\omega \tag{8}$$

for two-sided spectra. It is common to consider the power in a 1 Hz bandwidth. If $S_{\phi}(\omega)$ is constant over a 1 Hz bandwidth, (8) reduces to

$$\left[S_{\phi}(\omega) \Big|_{BW = 1\ Hz} = \overline{\phi^2(t)} \right] \tag{9}$$

The units of $S_{\phi}(\omega)$ are radians^2 per Hz bandwidth or more commonly expressed

as dB relative to 1 radian^2 per Hz bandwidth. By similar reasoning to the above, $S_{\dot{\phi}}(\omega)$ may be found to be

$$S_{\dot{\phi}}(\omega)\Big|_{BW = 1\ Hz} = \overline{\dot{\phi}^2(t)} \tag{10}$$

where the units of $S_{\dot{\phi}}(\omega)$ are $\left[\frac{(rad)}{(sec)}\right]^2$ per Hz bandwidth.

Since $\dot{\phi}(t)$ is the time derivative of $\phi(t)$ and since differentiation in the time domain is equivalent to multiplication by $j\omega$ in the frequency domain,

$$\left[S_{\dot{\phi}}(\omega) = \omega^2 \cdot S_{\phi}(\omega) \right] \tag{11}$$

$S_{\phi}(\omega)$ and $S_{\dot{\phi}}(\omega)$ are commonly referred to as "power" spectral densities (PSD), though there is no power involved in the units. Thus the units of $S_{\phi}(\omega)$ will sometimes be referred to as watts per Hz bandwidth.

B. Calculation of Oscillator Power Spectral Density (PSD)

Many attempts[4,5,6,7,8,9] have been made to arrive at a usable expression for the output spectrum of an oscillator. Perhaps the most quoted is the classic work of Edson[4,5]. Dr. Edson shows that in general noise perturbations in an oscillator result chiefly in phase or frequency disturbances and have only a second order effect on the amplitude of oscillation. Edson side-steps the difficult problem of nonlinearity by using a process of equivalent linearization and arrives at the conclusion that small nonlinearities result only in a reduction of $S_{AM}(\omega)$. Using a far more sophisticated nonlinear analysis, Hafner[7] arrives

at an expression for oscillator PSD which in general agrees with Edson[5] for small nonlinearity. Therefore based on the work of these investigators it is assumed that a relatively straightforward analysis will yield a close approximation for $S_{\phi}(\omega)$.

A simple block diagram representation of an oscillator is shown in Figure 1, where e_n represents all thermal and excess noise sources in the system

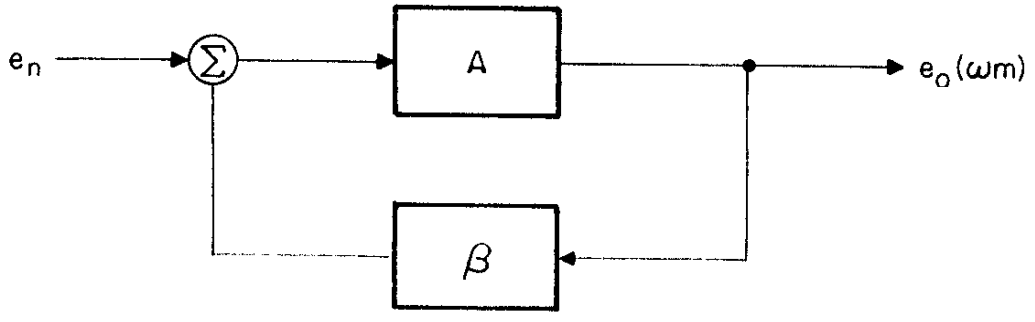

Figure 1
Oscillator Block Diagram

referenced to the input. $e_o(\omega_m)$ may be represented by

$$e_o(\omega_m) = \left(\frac{A}{1 - A\beta}\right) e_n \tag{12}$$

As the product $A\beta$ approaches unity, $e_o(\omega_m)$ increases without bound. In a practical oscillator however, nonlinearities limit the magnitude of $e_o(\omega_m)$ to a finite value such that the product $A\beta$ is slightly different from but very close to unity. Thus for sustained oscillation, $A \rightarrow 1/\beta$. If we assume that the feedback network is a single tuned circuit with a loaded quality factor of Q, β is given by

$$\left[\beta = \frac{1}{1 + j\,2Q\,\frac{\omega_m}{\omega_o}} \right] \tag{13}$$

At $\omega_m = 0$, $\beta = 1$, and thus $A \longrightarrow 1$. With this constraint

$$e_o(\omega_m) = \sqrt{1 + \left(\frac{\omega_o}{2\,Q\,\omega_m}\right)^2}\; e_n \qquad (\omega_m \neq 0) \tag{14}$$

The approximations used to derive (14) deteriorate as $\omega_m \longrightarrow 0$. At $\omega_m = 0$ (the frequency of oscillation) the value of $e_o(\omega_o) = e_s$ is determined by the output capabilities of the oscillator. Using the fact that the bandwidth (B) of a tuned circuit is equal to $\omega_o/2Q$, (14) may be expressed as

$$e_o(\omega_m) = \sqrt{1 + (B/\omega_m)^2}\; e_n \qquad (\omega_m \neq 0) \tag{15}$$

Thus for ω_m within the bandwidth of the tuned circuit,

$$e_o(\omega_m) \approx \frac{B}{\omega_m}\, e_n \qquad (\omega_m < B) \tag{16}$$

For ω_m outside of the bandwidth,

$$e_o(\omega_m) \approx e_n \qquad (\omega_m > B) \tag{17}$$

Thus the feedback network increases the noise output within its bandwidth. For frequencies outside of the bandwidth, the feedback is out of the circuit and since $A \approx 1$, the noise voltage output is identical to the equivalent amplifier

noise input voltage, e_n, given by*

$$e_n = \sqrt{FkTR_{in}} \quad \text{(effective volts/}\sqrt{\text{Hz BW}}\text{)} \tag{18}$$

where;

F = effective noise figure

k = Boltzmann's constant (1.38×10^{-23})

R_{in} = amplifier input resistance

The signal input power, P_s, is $(e_s)^2/R_{in}$. Thus the input noise to signal power ratio is

$$(NSR)_{in} = \frac{FkT}{P_s} \quad \text{(per Hz BW)} \tag{19}$$

The output noise to signal power ratio is equal to (19) times the square of the voltage transfer ratio. Using (14);

$$(NSR)_{out} = \left[1 + \left(\frac{\omega_o}{2Q\,\omega_m} \right)^2 \right] \frac{FkT}{P_s} \quad \text{(per Hz BW)} \tag{20}$$

Again assuming phase noise to be the controlling phenomenon, $S_\phi(\omega_m)$ may be obtained as twice the value of $(NSR)_{out}$ obtained from (20). A factor of two is required since $S_\phi(\omega_m)$ is defined for two-sided spectra. Thus

$$S_\phi(\omega_m) = \left[1 + \left(\frac{\omega_o}{2Q\,\omega_m} \right)^2 \right] \frac{2FkT}{P_s} \quad \text{(per Hz BW)} \tag{21}$$

---

* All thermal and excess noise sources are assumed to have a Gaussian amplitude distribution and a flat or "white" frequency spectrum.

As before this can be broken into two components,

$$S_{\phi}(\omega_m < B) \approx \left(\frac{\omega_o}{2Q\,\omega_m}\right)^2 \frac{2FkT}{P_s} \quad \text{(per Hz BW)} \tag{22}$$

$$S_{\phi}(\omega_m > B) \approx \frac{2FkT}{P_s} \quad \text{(per Hz BW)} \tag{23}$$

The following conclusions may be drawn from (21);

1) The noise should decrease at 6 dB/octave as Q increases or as ω_m increases (for $\omega_m < B$).

2) The noise should increase at 6 dB/octave as ω_o increases.

3) The noise figure adds directly to the output noise.

4) Increasing oscillator feedback power should decrease phase noise.

In order to test the validity of (21), several oscillators available in the laboratory were measured using the measurement technique outlined in the Appendix. The results are shown in Figures 2, 3, and 4. The following comments are in order regarding the results.

1) As assumed, the AM noise component is far below the phase noise for all of the oscillators tested.

2) At values of ω_m less than 10 kHz the curves rise on a much higher slope than the predicted 6 dB/octave.

3) Figure 3 (the only oscillator for which approximate design data was available) demonstrates the validity of (21) for ω_m greater than 20 kHz.

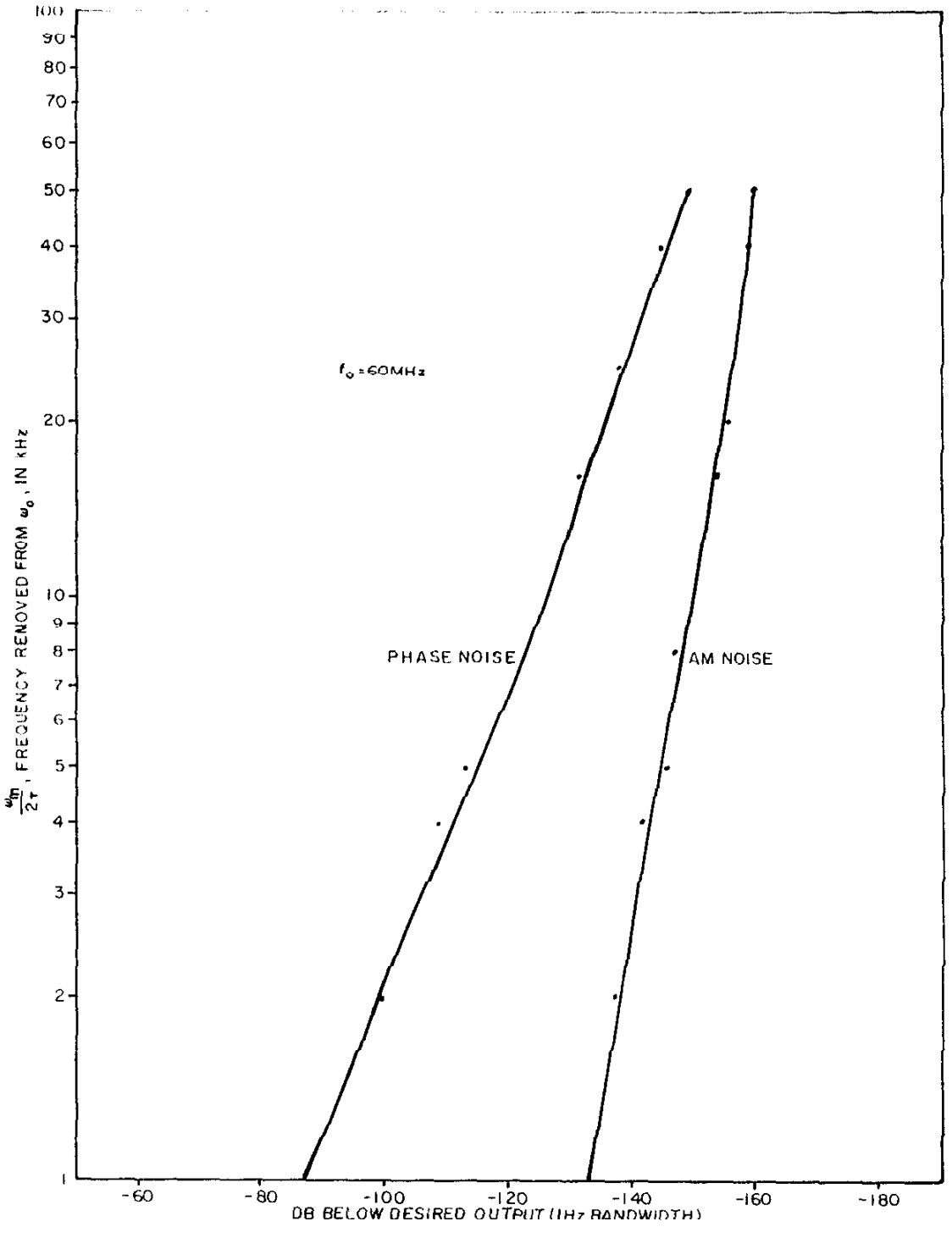

Fig. 2 PSD Curves for H-P Model 606A Signal Generator (SER #038-02481)

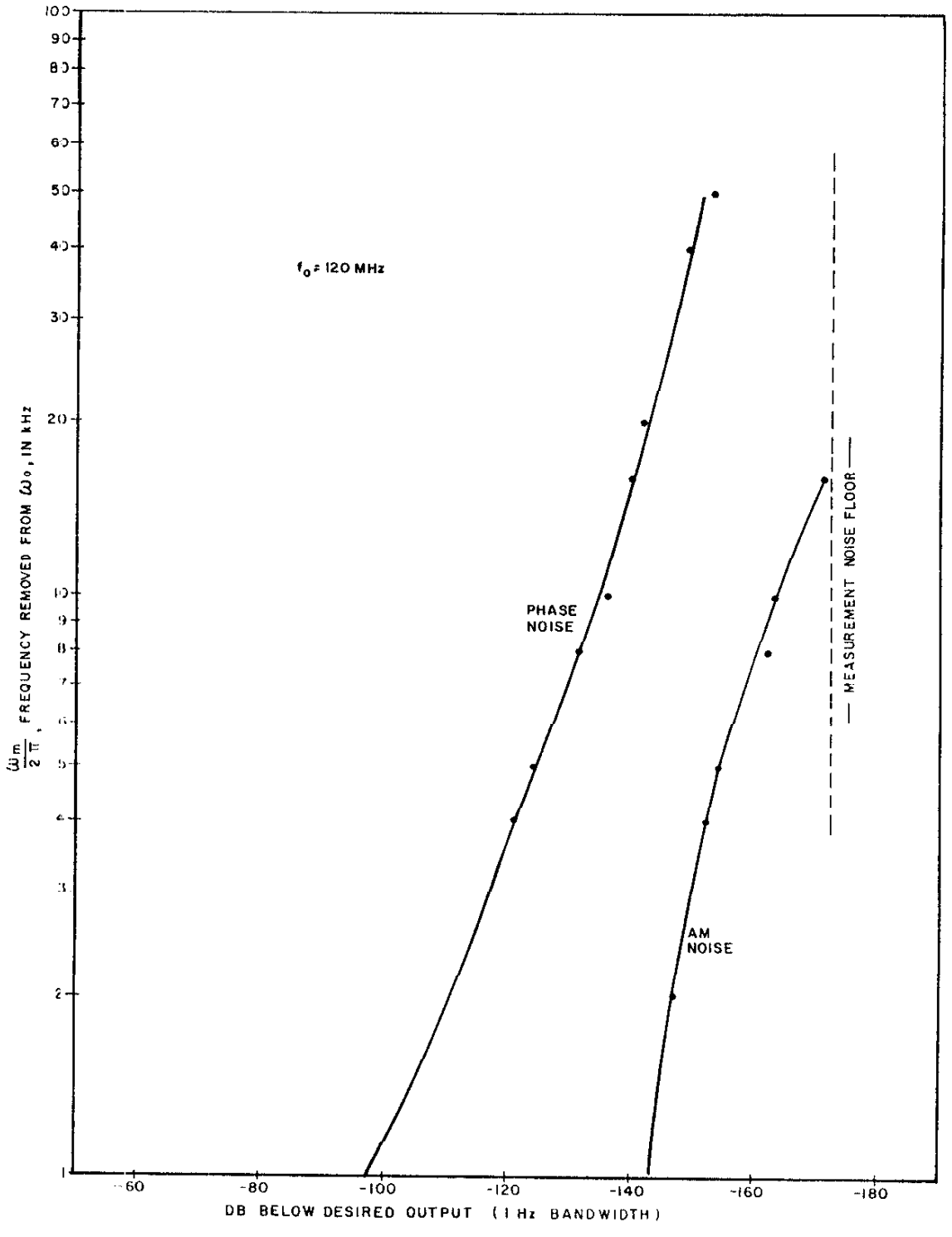

Fig. 3 PSD Curves for H-P Model 608-C Signal Generator (SER #010-03201)

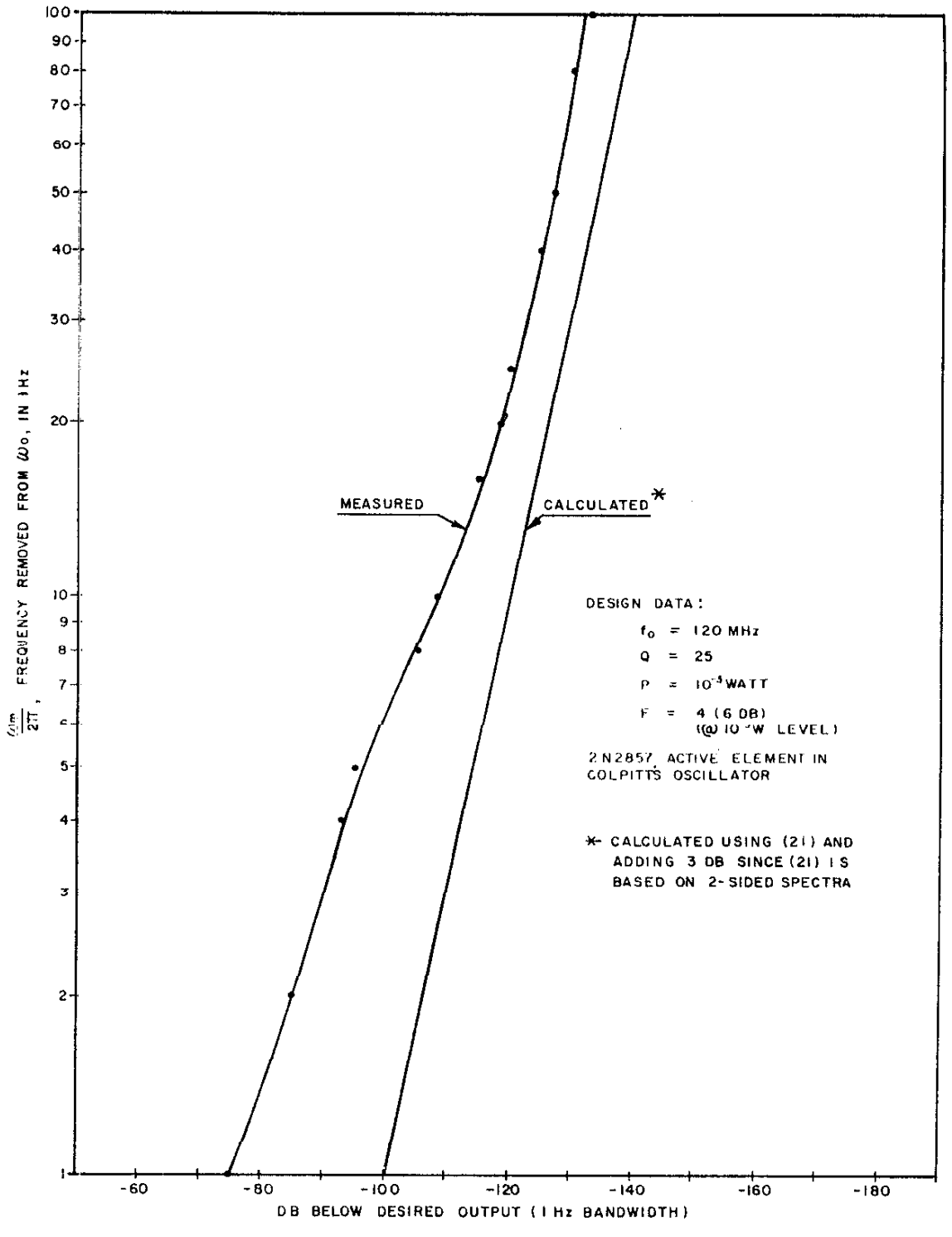

Fig. 4 PSD Curve for Breadboard VFO Phase Noise

The discrepancy noted in 2 above has been described by Leeson[6], and is believed to be due to 1/f parameter variations which give rise to a 9 dB/octave slope for lower values of ω_m where these effects predominate.

C. Oscillator Equivalent Circuit

The simplified block diagram (Figure 1) used to generate the expression for the oscillator power spectral density (PSD) is not suitable for use as a practical design tool. In the present section a more definitized equivalent circuit will be analyzed to allow optimization of the oscillator circuit.

Consider the circuit of Figure 5,

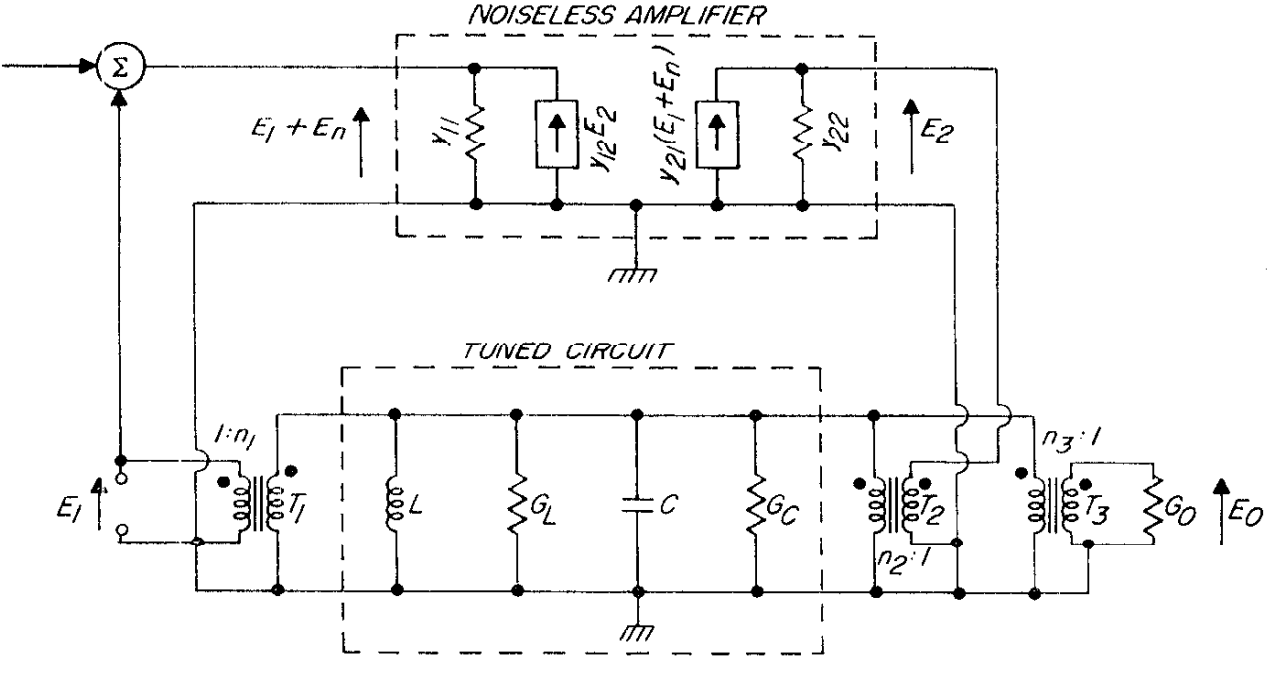

Figure 5

Oscillator Equivalent Circuit

where,

$E_n = \sqrt{\frac{FKT}{G_{11}}}$ = equivalent RMS noise voltage per root Hz at the amplifier input. (Hafner[10] has established that all oscillator noise sources are essentially equivalent and may be represented by a single equivalent noise source).

y_{11} = amplifier input admittance

y_{21} = amplifier forward transadmittance

y_{12} = amplifier reverse transadmittance

y_{22} = amplifier output admittance

G_L = inductor unloaded conductance

G_c = capacitor unloaded conductance

G_o = load conductance

T_1, T_2 and T_3 are ideal transformers. In a practical circuit these are replaced by capacitance (Colpitts) or inductive (Hartley) taps on the tuned circuit without loss of generality. To simplify the analysis, the amplifier self and mutual admittances will be assumed real. This is equivalent to absorbing the reactive components into the tuned circuit and representing the total effect as single lumped L and C components. By similar reasoning it is easily shown (if $y_{12} << y_{21}$) that y_{12} may be assumed equal to zero, resulting only in a slight change in the value of n_1 and n_2 necessary for sustained oscillation. A more

workable equivalent circuit is thus generated as shown in Figure 6. The load conductance has been absorbed into G_u.

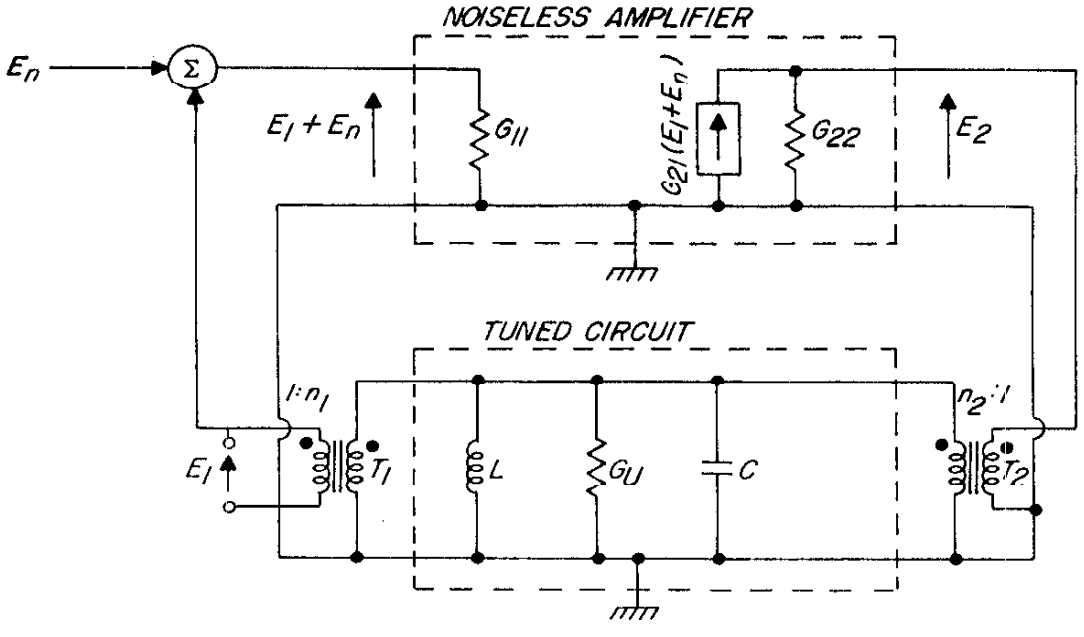

Figure 6

Simplified Equivalent Circuit

Here,

G_{11} = amplifier input conductance

G_{21} = amplifier forward transconductance

G_{22} = amplifier output conductance

$G_u = G_r + G_c + \dfrac{G_o}{n_3^2}$

An equivalent two-terminal oscillator may be generated by transforming all conductances and the current generator through T_1, T_2, and T_3 as shown in

Figure 7.

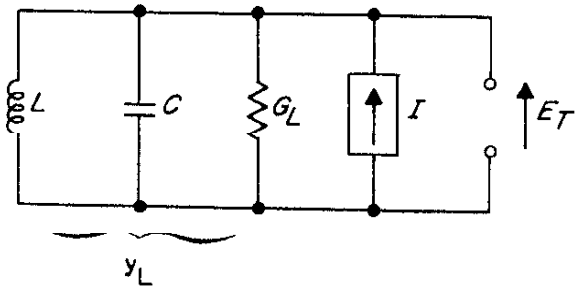

Figure 7

Two Terminal Oscillator

where,

$$G_L = G_u + \frac{G_{11}}{n_1^2} + \frac{G_{22}}{n_2^2} = \text{total loaded conductance}$$

$$I = \frac{G_{21}(E_1 + E_n)}{n_2} \tag{24}$$

The tank voltage, E_t, due to the input noise is;

$$E_t = \frac{I}{y_L} = \frac{G_{21}(E_1 + E_n)}{n_2\left[G_L + j\left(\omega C - \frac{1}{\omega L}\right)\right]} \tag{25}$$

Letting $\omega = \omega_o + \omega_m$, where $\omega_m << \omega_o$, and transforming variables;

$$E_t(\omega_m) = \frac{G_{21}(E_1 + E_n)}{n_2 G_L\left(1 + j2Q\frac{\omega_m}{\omega_o}\right)} \tag{26}$$

From Figure 6,

$$E_1 = \frac{E_t}{n_1} \tag{27}$$

Solving (26) and (27) for $E_t(\omega_m)$ yields,

$$E_t(\omega_m) = \frac{G_{21}\ E_n}{n_2\ G_L\ (1 + j2Q\ \frac{\omega_m}{\omega_o}) - \frac{G_{21}}{n_1}} \tag{28}$$

At $\omega_m = 0$ $(\omega = \omega_o)$;

$$E_t(0) = \frac{G_{21}\ E_n}{n_2\ G_L - \frac{G_{21}}{n_1}} \tag{29}$$

For sustained oscillation, $E_t(0) \gg E_n$, and therefore,

$$n_2\ G_L \longrightarrow \frac{G_{21}}{n_1} \qquad \text{or } n_1\ n_2\ G_L \longrightarrow G_{21} \tag{30}$$

Under this constraint, (28) becomes

$$E_t(\omega_m) = \frac{n_1\ E_n}{j2Q\ \frac{\omega_m}{\omega_o}} \qquad (\omega_m \neq 0) \tag{31}$$

The oscillator noise-to-signal ratio (NSR) is equal to the magnitude of the ratio of the mean square noise voltage, $E_t^2(\omega_m)$ to the mean square signal voltage, E^2_{TS};

$$NSR = \left| \frac{E_t^2(\omega_m)}{E_{TS}^2} \right| = \left(\frac{\omega_o}{2Q\omega_m} \right)^2 \frac{n_1^2\ E_n^2}{E_{TS}^2} \qquad (\omega_m \neq 0) \tag{32}$$

As before $S_\phi(\omega_m)$ may be obtained as twice this value, or

$$S_\phi(\omega_m) = \left(\frac{\omega_o}{2Q\omega_m}\right)^2 \frac{2\ n_1^2\ E_n^2}{E^2_{TS}} \qquad (\omega_m \neq 0) \tag{33}$$

This may be converted into more familiar form by noting that $E_n = \sqrt{\frac{FKT}{G_{11}}}$ (per root Hz), and $E_{IS} = \frac{E_{TS}}{n_1}$ = signal input voltage to amplifier;

$$S_\phi(\omega_m) = \left(\frac{\omega_o}{2Q\,\omega_m}\right)^2 \frac{2\,FKT}{G_{11}\,E_{IS}^2} \text{ (per Hz BW) } (\omega_m \neq 0) \qquad (34)$$

But $G_{11}\,E_{IS}^2 = P_s$ = signal power input to amplifier. Thus,

$$\left[S_\phi(\omega_m) = \left(\frac{\omega_o}{2Q\,\omega_m}\right)^2 \left(\frac{2\,FKT}{P_s}\right) \text{ (per Hz BW) } (\omega_m \neq 0) \right] \qquad (35)$$

which is identical to equation 22. However (22) was valid only within the bandwidth of the tuned circuit whereas (35) is not so restricted. This result was anticipated by Leeson[11] and is due to the fact that the output is taken from directly across a parallel resonant tuned circuit rather than the output of an amplifier with a series resonant tuned circuit in a feedback path (as used to derive Equation 22).

Equation (35) indicates that $S_\phi(\omega_m)$ tends to zero as ω_m is increased. Actually the minimum value is limited by thermal noise at the output (not considered in the analysis) and by the noise figure of the following stages.

II. OSCILLATOR DESIGN OPTIMIZATION

Using Equation (35) as a design guide it is possible to formulate some qualitative "rules of thumb" regarding oscillator noise performance. For a given oscillator frequency (ω_o) and a given frequency removed (ω_m) (these are usually specified or known), three factors control the oscillator noise spectrum;

1) F, the noise figure of the active element
2) P_{in}, the signal input power to the active element
3) Q, the loaded, or effective, Q of the tuned circuit

These factors are not usually completely independent. For example the noise figure of a bi-polar transistor is a function of the emitter current, which in turn is determined by P_{in}. P_{in} and Q are inter-related due to the loading effect on the tuned circuit of the active stage input impedance.

In order to proceed analytically it is necessary to choose a particular circuit with specified components, determine the functional inter-dependence of F, P_{in}, and Q, and then attempt to minimize $S_\phi(\omega)$. But how does one go about choosing a circuit as a reasonable starting point? A circuit which allows simultaneous minimization of F and maximization of P_{in} and Q is required. The type of oscillator (Hartley, Colpitts, etc.) is apparently not significant unless a particular configuration allows better optimization of the three design parameters.

Selection of an active device is a compromise between noise figure and power handling capability. Truly this is a problem of device dynamic range. Once the oscillator power level has been established, an active device which has the lowest noise figure at this power level is an optimum choice. Other device parameters such as gain and input and output impedances may be important, as they contribute to loading of the tuned circuit.

An attempt will be made in this section to arrive at a design procedure, whereby an optimum design may be established given specified parameters of the active element and the tuned circuit.

The problem of oscillator design optimization has received little attention in the literature. Most authors have limited their contributions to the analysis rather than the synthesis of oscillators. The synthesis of an optimum design, that is a design which will yield the lowest $S_{\phi}(\omega)$ for given parameters, is a formidable task because of the many different ways in which non-linearities may enter the problem. By making certain simplifying assumptions, however, it is possible to arrive at some general conclusions, at least for varactor tuned oscillators.

* The principle assumption to be made is that, for a varactor tuned oscillator, the limiting non-linearity is the amount of a-c signal voltage which may be impressed across the tuning varactors, thus limiting the oscillator power. Therefore it is tacitly assumed that an active element will be chosen which will handle the necessary power to keep the varactors as the limiting elements. A

secondary assumption is that the noise figure (F) of the active device is a constant and not a function of source impedance. This assumption is justified somewhat by the fact that the dependence of F on source impedance is very small, being nearly constant for wide variations of source impedance. Nevertheless it may be necessary to correct the value of F taking the source impedance into account.

From equation (34) and noting that $E_{TS} = n_1 E_{IS}$;

$$S_\phi(\omega) = \left(\frac{\omega_o}{2Q\,\omega_m}\right)^2 2\,FKT \left(\frac{n_1^2}{E_{TS}^2\,G_{11}}\right) \tag{36}$$

Since $Q = \frac{\omega_o C}{G_L}$, and $G_L = \frac{G_{21}}{n_1 n_2}$ (from 30);

$$S_\phi(\omega) = \frac{FKT\,G_{21}^2}{2(\omega_m C)^2\,E^2_{TS}\,G_{11}\,n_2^2} \tag{37}$$

For specified parameters, the only design variable in (37) is n_2^2. Obviously a minimum value of $S_\phi(\omega)$ is obtained by maximizing n_2^2.

From (30) and noting that $G_L = G_U + \frac{G_{11}}{n_1^2} + \frac{G_{22}}{n_2^2}$;

$$n_1 = \frac{G_{21} + \sqrt{G_{21}^2 - 4\,G_{11}\,G_{22} - 4\,n_2^2\,G_{11}\,G_U}}{2\left(n_2\,G_U + \frac{G_{22}}{n_2}\right)} \tag{38}$$

Since n_1 must be real and positive, the maximum value which n_2 may assume is that value which makes the radical vanish, $G_{21}^2 - 4G_{11}\,G_{22} = 4n_2^2\,G_{11}\,G_U$. Solving

for n_2:

$$n_{2OPT} = n_{2MAX} = \sqrt{\frac{G_{21}^2 - 4\,G_{11}\,G_{22}}{4\,G_{11}\,G_U}} \qquad (39)$$

Thus,

$$n_{1OPT} = \sqrt{\frac{G_{11}\,(G_{21}^2 - 4\,G_{11}\,G_{22})}{G_U\,G_{21}^2}} \qquad (40)$$

It is important to observe that this value of n_2 is the absolute maximum value which n_2 may assume for sustained oscillation. Thus in a practical oscillator n_2 must always be decreased somewhat from this value as a safety factor. Reducing n_2 by 30% results in an increase of $S_\phi(\omega)$ by approximately 3 dB.

Substitution of (39) into (37) and (36) yields the desired result;

$$S_\phi(\omega)_{OPT} = \frac{2\,FKT}{E_{TS}^2\,G_U}\left(\frac{\omega_o}{\omega_m\,Q_U}\right)^2\left(\frac{G_{21}^2}{G_{21}^2 - 4\,G_{11}\,G_{22}}\right) \qquad (41)$$

Two important conclusions may be drawn from (41);

1) If $G_{21}^2 \gg 4\,G_{11}\,G_{22}$, all of the active device parameters (G_{11}, G_{22}, G_{21}) except F drop out of the equation. Thus if this one condition is met, active elements for use in varactor-tuned oscillators may be judged solely on the merits of noise figure and power handling capability. However it is still necessary to use the optimum value for n_1 and n_2 (39 and 40) for each device in order to maintain this conclusion. Another interesting conclusion under this assumption (i.e., that $G_{21}^2 \gg 4\,G_{11}\,G_{22}$) may be drawn from (40), obtaining that $n_{1OPT} \approx \sqrt{\frac{G_{11}}{G_U}}$.

This is the condition of maximum power transfer from the tuned circuit to the input circuit of the active device, specifying an impedance match at the input.

2) $S_\phi(\omega)$ is inversely proportional to $Q_U^2 G_U$. Thus it is not only important to keep the unloaded Q as high as possible but also to keep G_U large. These conditions at first seem to be contradictory since Q_U and G_U follow an inverse relationship. Intuitively it is easy to see why Q_U should be large. The condition on G_U is brought about by the fact that E_{TS} is assumed to be limited to a maximum value by the varactor tuning voltage, and the oscillator tank power is thus limited only by the value of G_U.

In summary, an active device should be chosen with sufficient gain at the operating frequency, paying particular attention to the noise figure when operated with an impedance matched input at the chosen power level. A tuned circuit should be chosen which not only has a high unloaded Q, but optimizes the product $Q_U^2 G_U$. This latter requirement may be simplified further by referring to Figure 8.

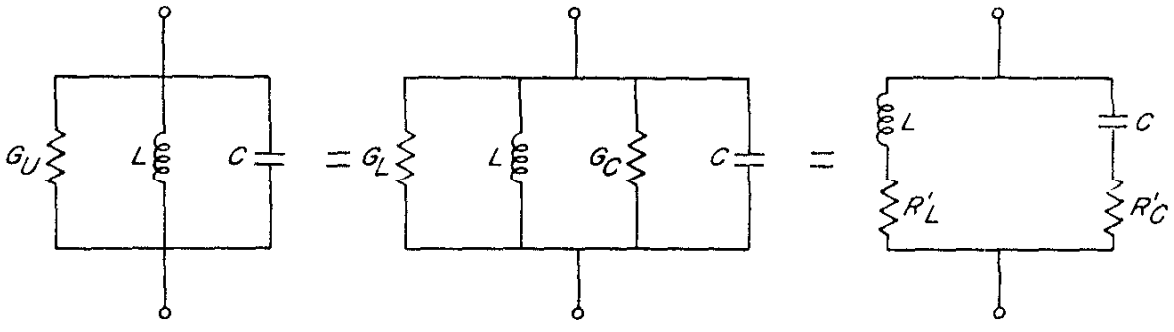

Figure 8

From the figure;

$$G_L = \frac{1}{(Q_U^2 + 1)\, R'_L} \approx \frac{1}{Q_U^2\, R'_L} \tag{42}$$

$$G_C = \frac{1}{(Q_U^2 + 1)\, R'_C} \approx \frac{1}{Q_U^2\, R'_C} \tag{43}$$

$$G_U = G_L + G_C \approx \frac{1}{Q_U^2} \left(\frac{1}{R'_L} + \frac{1}{R'_C} \right) \tag{44}$$

$$Q_U^2\, G_U \approx \left(\frac{1}{R'_L} + \frac{1}{R'_C} \right) = \frac{R'_L + R'_C}{R'_L\, R'_C} \tag{45}$$

The product $Q_U^2\, G_U$ is a maximum when R'_L and R'_C are minimum, and thus the requirement that $Q_U^2\, G_U$ be large is equivalent to requiring only that the series resistance of the tuned circuit components be as small as possible regardless of the L/C ratio (since neither L nor C appears in 45). This will normally be accomplished with a small L/C ratio (depending on frequency), i.e., a small inductance and a large capacitance.

It should be emphasized that these conclusions are only valid when the limiting non-linearity in the oscillator is the tuned-circuit tank voltage. Entirely different results would be obtained by assuming the limiting non-linearity to be associated with the active device. Also, although the tank voltage is the limited quantity, it must not be inferred that it is "self-limited", that is, saturating the varactors and driving them into forward conductance. Such operation would seriously affect the noise output of the oscillator. Instead, some type of automatic level control should be employed which will hold the tank voltage to the maximum permissable value.

III. 94.7 MHz TO 122.7 MHz OSCILLATOR

A. General Discussion

The preceding sections have dealt with analysis of the oscillator problem in general. In this section the results of this analysis will be applied to the design of a specific oscillator to meet the specifications outlined in the Introduction.

The oscillator must cover the frequency range of 94.7 to 122.7 MHz. Noise in a 1 Hz banswidth removed greater than 50 kHz from the oscillator frequency must be a minimum of 145 dB below the desired output $\left[S_{\phi}(\omega) = -142 \text{ dB} \right]$.

At this point it would be instructive to make a plot of $S_{\phi}(\omega)$ vs. F, P_{IN}, and Q to establish a reference starting point toward obtaining this goal. Let the standard conditions be:

$$S_{\phi}(\omega) = -142 \text{ dB}$$

$$\frac{\omega_o}{2\pi} = 100 \text{ MHz}$$

$$\frac{\omega_m}{2\pi} = 50 \text{ kHz}$$

$$T = 293^{\circ}K$$

Figure 9 is a plot of equation (35) under these assumptions. For other oscillator frequencies, ω'_o, it is necessary to add a correction factor of $20 \log_{10} (\frac{\omega_o}{\omega'_o})$ dB to $S_{\phi}(\omega)$.

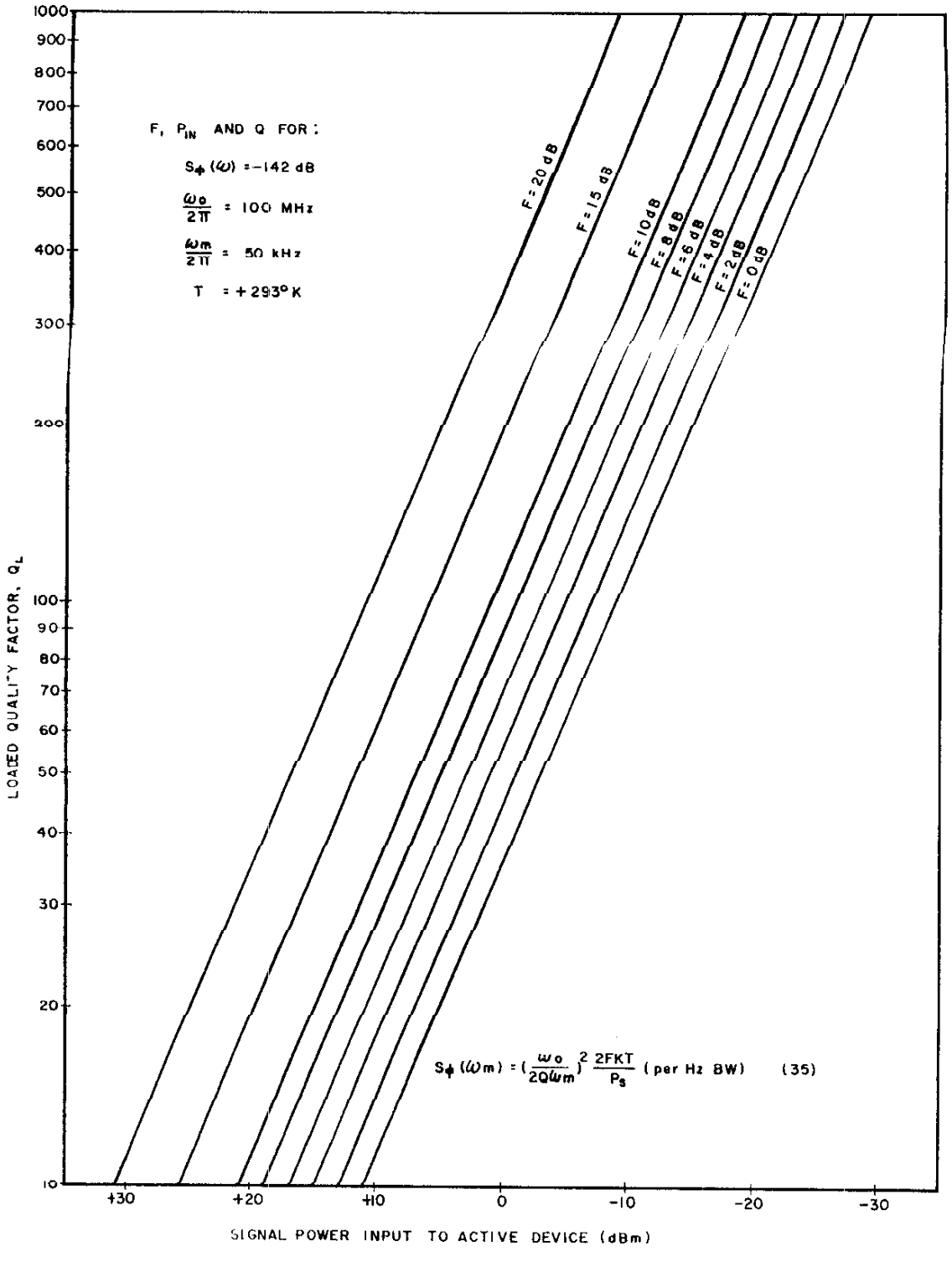

Fig. 9 Plot of Equation (35)

Figure 9 shows minimum values of F, P_{IN}, and Q to meet the specification. For example, with an effective noise figure of 6 dB and a power input to the active device of 0 dBm, an absolute minimum loaded Q of 71 is required with no design safety factor. These requirements are certainly within the present state of the art. Thus we will proceed to a design by choosing readily available components.

B. Helical Resonator

Design of the oscillator tuned circuit is not straightforward. The required oscillator frequency range (94.7 to 122.7 MHz) lies in the VHF "no-man's land" where high-Q tuned circuits are difficult to obtain with lumped components and cavity resonators are too large and bulky. Very high Q per unit volume in this range is obtainable from a helical line resonator[12], which is nothing more than a quarter-wave coaxial transmission line with a helically wound inner conductor with one end short-circuited. Tuning may be accomplished by varying a capacitance (by mechanical or electrical means) connected to the open-circuited end of the line. In this application, a voltage variable capacitor (varactor) will be considered for the tuning element as this is the simplest electronic tuning element available.

The basic helical resonator (fixed tuned) consists of a single-layer solenoid or helix enclosed in a conductive shield. The shield may in general have any shape, but this discussion will be limited to shields of square cross section. One end

of the helix is connected directly to the shield and the other end is open circuited. Figure 10 shows a sectional view of such a resonator.

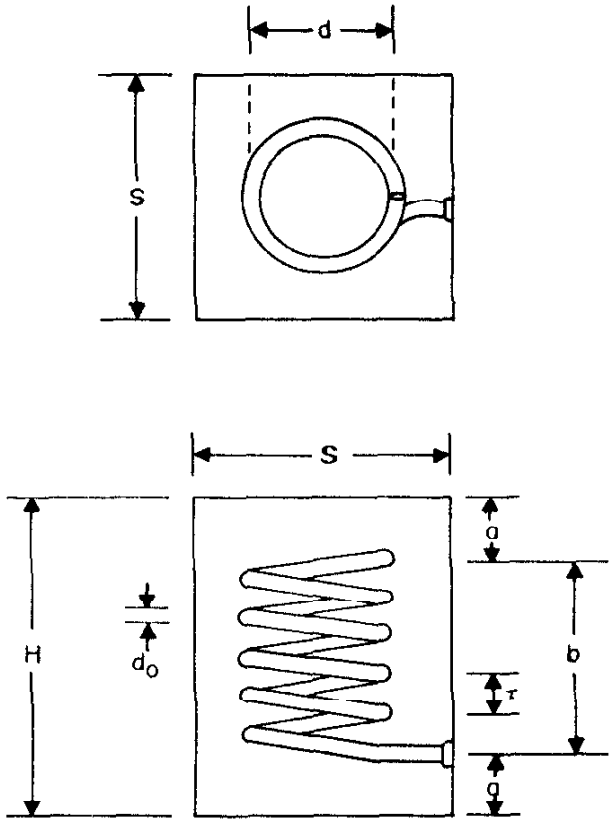

Figure 10

Helical Resonator Sectional View

where,

b = axial length of helix (inches)

d = mean diameter of helix (inches)

d_o = diameter of conductor (inches)

S = inside width of one side of square shield (inches)

n = pitch of helix (turns/inch)

N = total number of turns

H = length of shield (inches)

a = clearance of helix from ends of shield (inches)

Z_o = characteristic impedance of line (ohms)

With this notation the inductance, L, and capacitance, C, per unit length are given by[12];

$$L = 0.025\, n^2\, d^2 \left[1 - \left(\frac{d}{1.2\,S}\right)^2\right] \mu H/\text{axial inch} \tag{46}$$

$$C = \frac{0.75}{\log_{10} \frac{1.2\,S}{d}} \quad pf/\text{axial inch} \tag{47}$$

A convenient summary of helical resonator formulas is given by Zverev and Blinchikoff[13]. Certain relationships are empirically derived for optimizing unloaded Q. It is found that for maximum Q_u the following conditions should be maintained (approximately):

$$\frac{d}{s} = 0.66$$

$$b = S$$

$$H \quad 1.6\,S \text{ minimum} \tag{48}$$

$$d_o > 5\,\delta \quad (\delta = \text{skin depth})$$

$$a = 0.3\,S \text{ minimum}$$

Under these constraints, the following equations hold for a resonator at frequency f_o;

$$\begin{aligned} Q_u &= 6 \times 10^{-2} S \sqrt{f} \\ Z_o &= \frac{8.15 \times 10^{10}}{f_o S} \\ N &= \frac{1.6 \times 10^9}{f_o S} \\ n &= \frac{1}{\tau} = \frac{1.6 \times 10^9}{S^2 f_o} \end{aligned} \tag{48}$$

These relations are valid for a fixed-tuned resonator with no external tuning elements. The tuned frequency of the resonator may be lowered by connecting a capacitance between the open-circuited end of the helix and ground. To evaluate the relationship of this capacitance to the tuned frequency it is recalled that the admittance at the open circuited end of a shorted transmission line is given by;

$$Y_{sc} = \frac{\coth \gamma \xi}{Z_o} \tag{49}$$

where $\gamma = \alpha + j\beta$ = complex propagation constant

$$\alpha = \frac{\omega}{2 v_p Q_u} = \text{attenuation constant} \tag{50}$$

$$\beta = \frac{\omega}{v_p} = \text{phase constant} \tag{51}$$

$$\xi = 1.06\, b = \text{electrical length of line*} \tag{52}$$

* 6 percent higher than physical length due to fringing.

$$v_p = \frac{1}{\sqrt{LC}} = \text{velocity of propagation} \tag{53}$$

Accordingly;

$$Y_{sc} = \frac{1}{Z_o}\left[\frac{e^{2\alpha\xi} - e^{-2\alpha\xi}}{e^{2\alpha\xi} + e^{-2\alpha\xi} - 2\cos 2\beta\xi} - j\,\frac{2\sin 2\beta\xi}{e^{2\alpha\xi} + e^{-2\alpha\xi} - 2\cos 2\beta\xi}\right] \tag{54}$$

For very low loss lines such as the helical resonator, the attenuation constant, α, is very small. Under this condition Equation (54) reduces to;

$$Y_{sc} \approx \frac{1}{Z_o}\left[\frac{\alpha\xi}{\sin^2 \beta\xi} - j\cot\beta\xi\right] \tag{55}$$

The line is self-resonant (Y_{sc} is real) at $\omega = \omega_o$ when $\beta\xi = \pi/2 \pm n\pi$, the first (principal) resonance occurring at $\xi = \frac{\pi}{2\beta} = \frac{v_p}{4f_o}$ (quarter wavelength).

A line of fixed length ξ may be resonated at other frequencies by adding a susceptance equal to $-jIm\left[Y_{sc}\right]$ in parallel with the open-circuited end of the line, such that $Y_{eq} = Y_{sc} - jIm\left[Y_{sc}\right] = Re\left[Y_{sc}\right]$.

For $\omega < \omega_o$, Y_{sc} is inductive, and therefore a capacitance (C_p) of susceptance $B = Im\left[Y_{sc}\right]$ is required to make the line appear resonant at ω. Thus,

$$B = \omega C_p = \frac{\cot\beta\xi}{Z_o} = \frac{\cot\frac{\omega\xi}{v_p}}{Z_o} \tag{56}$$

and,

$$C_p = \frac{\cot\frac{\omega\xi}{v_p}}{\omega Z_o} \tag{57}$$

The resonator may be tuned over a band of frequencies, say from ω_1 to ω_2, by a variable capacitance with a range of C_1 to C_2, respectively. Of interest is the ratio C_1/C_2 when tuning from ω_1 to ω_2. By application of (57), and letting

$$\xi = \frac{v_p}{\lambda f_o} = \frac{\pi\, v_p}{2\,\omega_o} ;$$

$$\frac{C_1}{C_2} = \frac{(\omega_2)}{(\omega_1)} \times \frac{\left[\cot \left(\frac{\omega_1}{\omega_o} \times \frac{\pi}{2}\right)\right]}{\left[\cot \left(\frac{\omega_2}{\omega_o} \times \frac{\pi}{2}\right)\right]} \tag{58}$$

Figure 11 is a plot of Equation (58). $\frac{\omega_2}{\omega_o}$ is a measure of how close the upper tuned frequency is to the self-resonant frequency. Figure 11 shows that the tuning capacitance ratio C_1/C_2 increases without bound as $\frac{\omega_2}{\omega_o}$ approaches 1. This occurs since $C_2 \to 0$ at $\omega_2 = \omega_o$. Thus in a practical situation it is necessary to keep ω_2 less than approximately 70% of ω_o to keep the capacitance ratio from becoming excessive. On the other hand as $\frac{\omega_2}{\omega_o}$ is lowered, the actual capacitance of C_1 and C_2 increases, even though the ratio C_1/C_2 decreases. This added capacitance has a detrimental effect on the Q of the resonator (The Q is a maximum under conditions of self-resonance where the tuned circuit is completely distributed). Thus ω_2 should be kept as close to ω_o as possible, consistent with the constraints on C_1/C_2 in Figure 11. C_1 and C_2 represent the total added external capacitance including circuit and wiring strays.

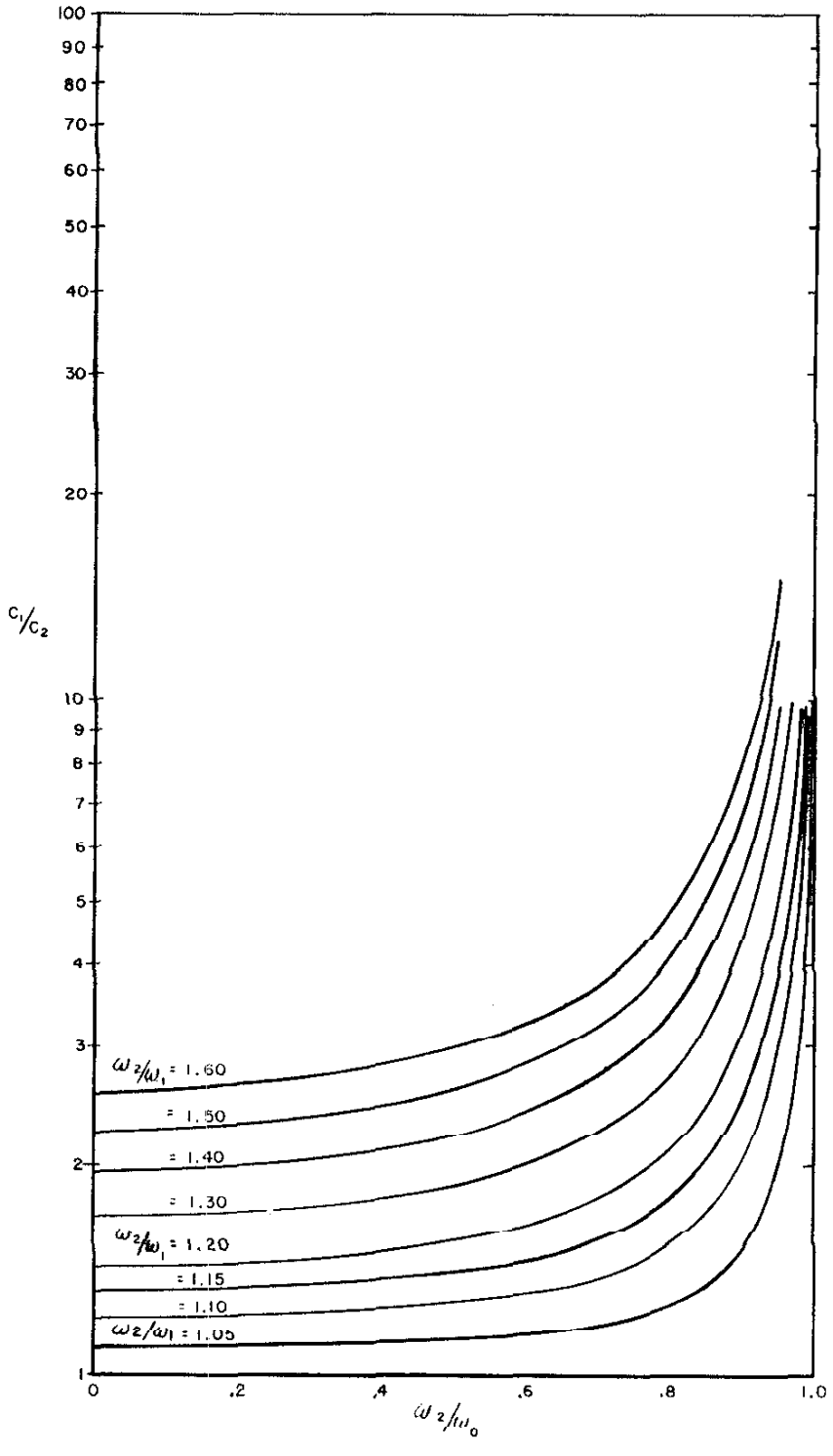

Fig. 11 C_1/C_2 vs ω_2/ω_o

C. Varactor Tuning

In the frequency range of interest (94.7 to 122.7 MHz) a resonator of one square inch cross-sectional area (S = 1 inch) yields an unloaded Q of approximately 600 (Equation 48). To maintain a high Q while tuning over the band, very high Q varactors are required. These devices utilize the capacitance of a reverse-biased p-n junction. As the reverse bias voltage is increased, the depletion layer width increases thus separating the "plates" of the capacitor and decreasing the junction capacitance. Only recently have high Q varactors become available for use in the VHF region. The Motorola MV1864B is representative of the present state of the art in high Q devices. Figure 12 shows the equivalent circuit of the MV1864B, and Figure 13 shows a simplified circuit which is very accurate in the desired frequency range.

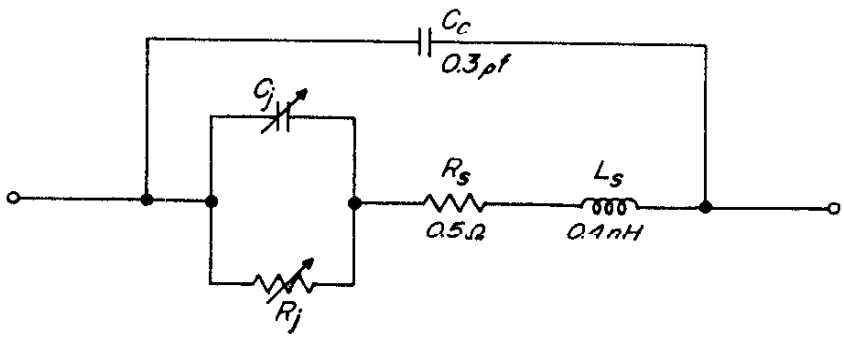

C_j: Voltage — variable junction capacitance

R_j: Voltage — variable junction resistance (negligible above 100 kHz)

R_s: Series resistance (semiconductor bulk, contact, and lead resistance)

C_c: Case capacitance

L_s: Series inductance

Figure 12

Varactor Equivalent Circuit

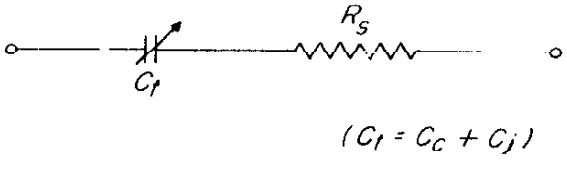

Figure 13

Simplified Varactor Equivalent Circuit

C_j may be expressed as;

$$C_j = \frac{C_o}{(1 + \frac{V_r}{\phi})^n} \tag{59}$$

where;

V_r = applied reverse bias voltage

ϕ = diffusion potential ($\approx$ 0.6 volt)

C_o = C_j at $V_r = 0$

n = exponent $\approx$ 0.5 (abrupt junction)

The Q of the device is given approximately by:

$$Q = \frac{1}{\omega C_t R_s} \tag{60}$$

Since C_t and R_s are nearly independent of frequency, Q is a linearly decreasing function of ω. C_t is approximately (except at very low tuning voltages) inversely proportional to the square root of applied voltage, thus making Q a square root function of applied voltage. Typical characteristics of the MV1864B are shown in Figures 14 and 15.

A fundamental limitation of the use of varactors in this application is the amount of signal voltage (a-c swing) which may be superimposed on the quiescent d-c bias voltage without deleterious effects on the oscillator performance. The oscillator noise degradation due to parametric pumping of the varactors will be discussed later. Obviously the peak a-c voltage swing cannot be greater than

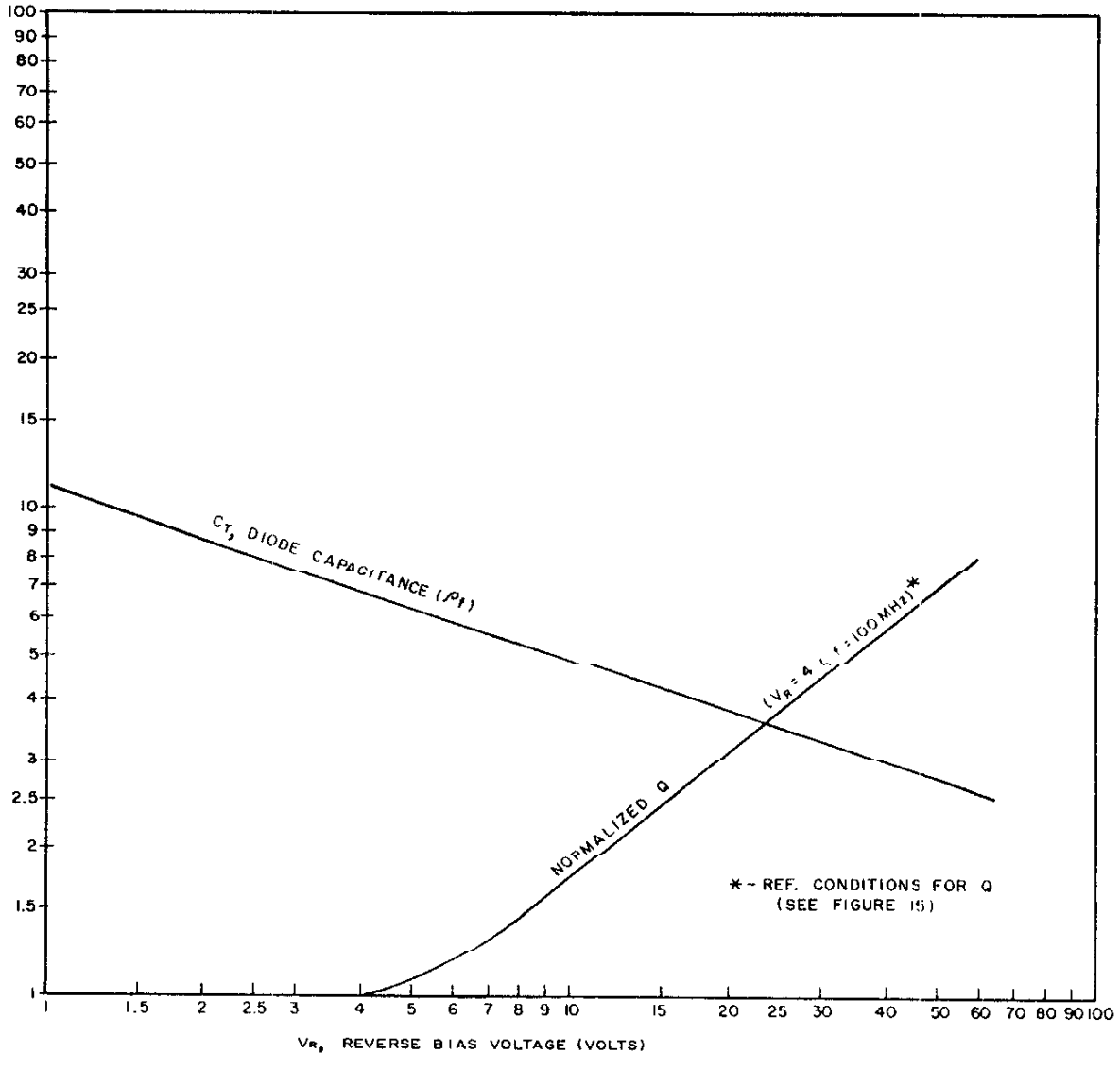

Fig. 14 Motorola MV1864 B Capacitance & Q vs Bias Voltage Typical Characteristics

Fig. 15 Motorola MV1864 B Q vs Frequency Typical Characteristics

the bias voltage as this would result in forward biasing of the varactor. In addition to generating excess noise in the diode, this would cause shunting of the tuned circuit by a low impedance over a portion of the cycle, seriously affecting the Q. A similar situation exists when the bias voltage nears the reverse breakdown voltage of the varactor. The peak voltage swing must not be high enough to cause avalanching. These problems may be avoided in a practical situation by;

1) keeping the a-c voltage swing low;

2) limiting the bias voltage excursion to medium values, avoiding very low and very high tuning voltages;

3) connecting several varactors in series to lower the a-c swing across each one.

In this design application, the a-c voltage swing cannot arbitrarily be lowered since this would require either lowering of the Q or the oscillator power input, thus increasing the relative noise output. The bias voltage excursion may be limited somewhat, but the capacitance ratio from the lowest to the highest tuning voltage must be sufficient to allow tuning the desired frequency range (Figure 11). The series connection of varactors is economically inefficient if it is necessary to maintain the same effective capacitance across the ends. The total capacitance of n varactors in series each of capacitance C_t, is $\frac{C_t}{n}$ and the voltage across each diode is reduced by a factor of n. n of these series interconnections connected in parallel are required to regain a total capacitance of

C_t. Thus n^2 varactors are required to reduce the voltage across each diode by a factor of n. (This assumes equal quiescent d-c biasing of all diodes.) When making series interconnections of varactors it is desirable to alternate the polarity such as shown in Figure 16. This results in a significant reduction in the overall capacitance nonlinearity as a function of instantaneous applied signal voltage since for a given rate of change of applied voltage, half of the varactors are increasing capacitance (the applied voltage is bucking the quiescent bias) while the other half are decreasing capacitance (the applied voltage is aiding the quiescent bias).

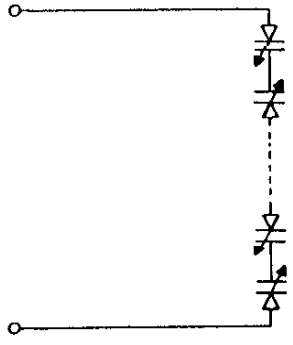

Figure 16

Equivalent A-C Circuit Back-To-Back Series Connection

D. Breadboard Oscillator

A breadboard varactor tuned helical resonator oscillator was designed and fabricated as follows. A helix with a one inch square cross-sectional shield (S = 1") was chosen as a convenient starting point, since this results in a resonator Q of approximately 600, sufficient to keep the varactors as the

Q-controlling element.

Refer to Figure 11. The required tuning ratio (ω_2/ω_1) is 122.7/94.7 $\approx$ 1.30. Choosing a ω_2/ω_0 ratio of 0.70 (see discussion following Equation 58) results in a self-resonant frequency of ω_0 = 122.7/0.7 = 175 MHz. From Equation (46) to (57);

d	=	mean diameter of helix	=	0.66 inch
b	=	axial length of helix	=	1.0 inch
H	=	length of shield	=	1.6 inches
a	=	end clearance	=	0.3 inch minimum
N	=	total number of turns	=	9.15
n	=	pitch of helix	=	9.15 turns/inch
L	=	line inductance	=	0.636 μH/inch
C	=	line capacitance	=	2.88 ρf/inch
Z_o	=	characteristic impedance	=	465 ohms
v_p	=	velocity of propagation	=	7.4×10^8 inches/sec.
Q_u	=	unloaded Q of helix	=	$6 \times 10^{-2} \sqrt{f}$
α	=	attenuation constant	=	$7.08 \times 10^{-8} \sqrt{f}$ rad/inch
β	=	phase constant	=	8.48×10^{-9} f rad/inch
ξ	=	electrical length of helix	=	1.06 inches
$\mathrm{Re}\left[y_{sc}\right]$	=	conductance of helix = G_r	=	$\dfrac{1.61 \times 10^{-10} \sqrt{f}}{\sin^2 (8.9 \times 10^{-9} f)}$
C_1	=	tuning C at 94.7 MHz	=	3.18 ρf
C_2	=	tuning C at 122.7 MHz	=	1.42 ρf

Thus a tuning capacitance ratio of 3.18/1.42 = 2.24 is required. These capacitances must include all circuit and wiring strays. Since it is very difficult to estimate such small values of stray capacitance accurately, it was decided to proceed with the fabrication of a breadboard oscillator.

The Motorola MV 1864B varactor tunes the required capacitance ratio between approximately 5 and 55 volts with an absolute capacitance of twice the required value. Thus two diodes in series provide the correct capacitance as shown in Figure 17.

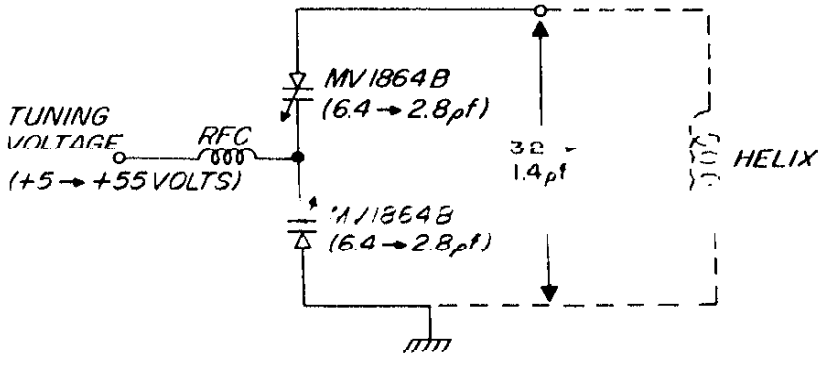

Figure 17

Two Diode Configuration

This configuration limits the peak signal swing to an absolute maximum of 10 volts. To allow greater voltage excursions it was decided to stack the varactors as shown in Figure 18. This configuration doubles the allowable peak swing.

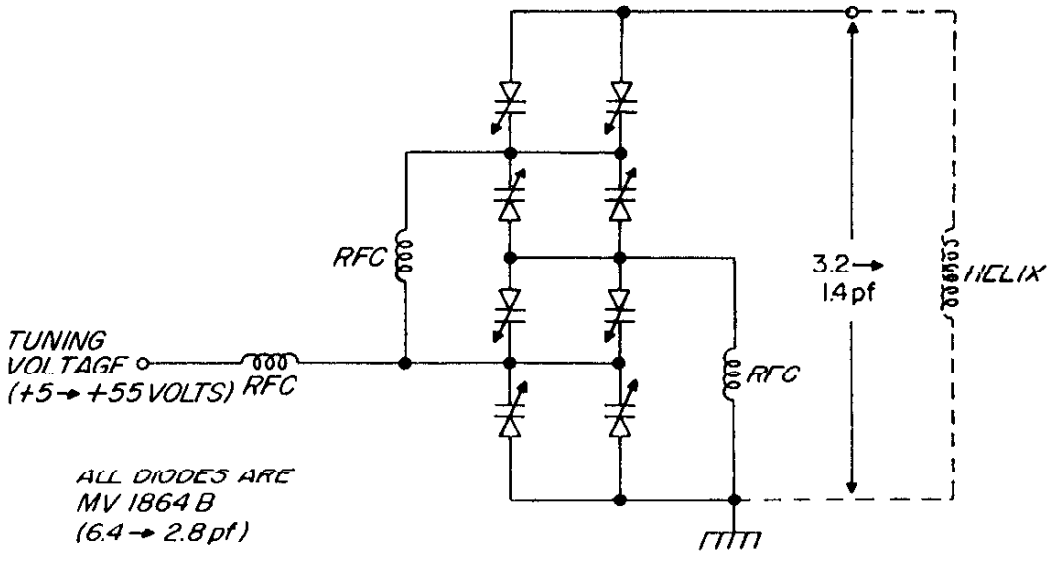

Fig. 18 Eight Diode Configuration

The r-f chokes shown in Figure 18 are arranged such that the impedance of any one choke is reflected to the helix by a ratio of at least 4:1. These chokes proved to be very difficult to design in order to prevent loading of the circuit or other undesirable effects. An r-f resistance of 100,000 ohms minimum and a reactive component of less than 0.1 pf was the desired goal. The use of resistors was ruled out because of the generated noise voltage which they impress across the varactors, which in turn phase modulate the oscillator. After some experimentation it was found that a self-resonant choke offered the best compromise. 70 turns of No. 39 wire on a 1/8" diameter, 3/8" long form proved to be an optimum choice, with a self-resonant frequency of approximately 110 MHz. The r-f resistance of these chokes was found to remain above 150,000 ohms and the capacitance between 0.15 pf across the oscillator frequency range.

The design of the tuned circuit is thus complete. It remains to tabulate the conductance at the top of the helix for the helix-varactor combination.

		Conductance (micro-mhos) 94.7 MHz	122.7 MHz
$G_r = R_e\left[Y_{sc}\right]$	=	2.77	2.24
G_o = (See Figures 14 and 15)	=	4.31	0.43
G due to r-f chokes	=	2.50	2.50
Total G	=	*9.58*	*5.17*

This represents the unloaded shunt conductance of all of the tuned circuit components referenced to the top of the helix. The unloaded Q may be calculated

after consideration of the output loading, since the output load was included in the analysis as part of the unloaded Q of the oscillator. (The oscillator loaded Q was taken as the operating Q with the oscillator active element connected.)

An optimum output connection would be one which loaded the tuned circuit only slightly, yet extracted sufficient power to maintain the output signal-to-noise ratio. A device well suited for this application is a field-effect transistor (FET) in a common source connection. The Union Carbide type 2N4416 is typical of the state of the art in VHF FET's. This device has a noise figure of less than 2 dB at 100 MHz when fed from a source impedance of 500 ohms (at 200 milli-watt dissipation level). Under these conditions the input impedance is greater than 10K. Thus this device may be used to extract signal from the oscillator while at the same time causing very little loading. In the breadboard oscillator a common source 2N4416 amplifier was tapped into the helix at approximately 1 turn. The reflected load at the top of the helix was estimated to be $(9.15)^2 \times 10^4$ = 837K (1.2 micro-mhos).

The total unloaded conductance is thus 9.58 + 1.20 = 10.78 micro-mhos at 94.7 MHz and 5.17 + 1.20 = 6.37 micro-mhos at 122.7 MHz. The unloaded Q is $\frac{1}{2\pi f L G}$;

$$Q_u \text{ (94.7 MHz)} = 245$$

$$Q_u \text{ (122.7 MHz)} = 320$$

The 2N4416 was also chosen for use in the oscillator because of its low noise

figure at relatively high operating power. A common gate connection was used for the oscillator because in this connection the noise figure is optimum with an impedance matched input (see discussion following equation 41). Also the input and output voltages are in phase, allowing feedback to be accomplished by simply tapping the helix.

A Hartley configuration was used to minimize stray capacitance. A schematic of the breadboard oscillator-buffer is shown in Figure 19. Resistor R_3 limits the average current in oscillator transistor Q_2 and provides the limiting action needed to control the power level of the oscillator and prevent saturation of the varactors. A current limiter of this type was found to be superior to any sort of voltage limiting which tended to load the circuit by presenting a low impedance over part of the cycle.

The optimum tap positions for the source and drain of Q_2 may be determined from equations (39) and (40):

$$n_{2_{max}} = \sqrt{\frac{G_{21}^2 - 4\,G_{11}\,G_{22}}{4\,G_{11}\,G_u}}$$

$$n_1 = \sqrt{\frac{G_{11}\,(G_{21}^2 - 4\,G_{11}\,G_{22})}{G_u\,G_{21}^2}}$$

For the common-gate connection, $G_{11} \approx G_{21}$, and these relations simplify to

$$n_{2_{max}} = \sqrt{\frac{G_{21} - 4\,G_{22}}{4\,G_u}} \quad ; \quad n_1 = \sqrt{\frac{G_{21} - 4\,G_{22}}{G_u}}$$

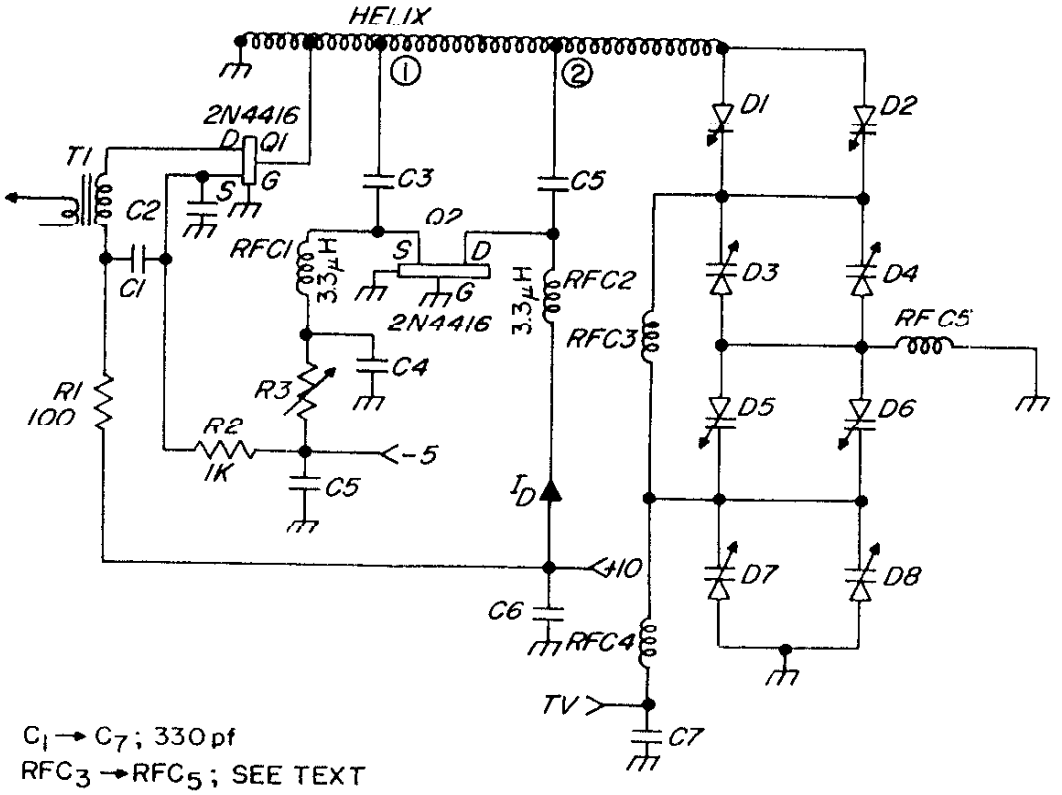

$C_1 \rightarrow C_7$; 330 pf
$RFC_3 \rightarrow RFC_5$; SEE TEXT
$D_1 \rightarrow D_8$; MV 1864 β
T_1; 50 Ω BALUN

Fig. 19 Breadboard Oscillator Schematic

The transistor parameters are a function of the operating point, which may be determined graphically by reference to Figure 20. These curves represent typical characteristics for G_{21} at 1 kHz at 25°C. To allow for device variation, frequency roll off and temperature, values for G_{21} should be reduced by approximately 40%. G_{22} may be assumed constant at 30 micro-mhos. The largest value of G_u occurs at 94.7 MHz (G_u = 10.8 micro-mhos).

First trial calculation: Assume operation at I_{DSS} = 10 ma (V_{gs} = 0) and V_{DS} = +10 volts. From the figure, $G_{21} = G_{11}$ = 5100 micro-mhos (less 40% ≈ 3100 micro-mhos). Thus,

$$n_{2max} = \sqrt{\frac{3100 - 4(30)}{4(10.8)}} = 8.3$$

To assure sustained oscillation, n_2 should be reduced by approximately 30% (see discussion following equation 40). Let n_2 = 5.8. The minimum tuning voltage on the varactors is 5 volts.

Since 4 diode pairs are used in series, the peak tank voltage must be less than 20 volts. Let the peak allowable tank voltage be 15 volts. Then the peak allowable signal voltage at the transistor drain is $V_{pd} = \frac{15}{5.8} = 2.59$ volts. The drain is operating into a load conductance of $G_{dl} = 2\, n_2^2\, G_u$ (an impedance match is assumed at the transistor input). Thus, $G_{dl} = (2)\ (5.7)^2\ (10.8) = 702$ micro mhos. Assuming Class A (linear) operation, the peak allowable drain signal current is $I_{pd} = (V_{pd})\ (G_{dl}) = 1.82$ ma. Since current limiting is to be employed, a second trial calculation will be made using a quiescent drain

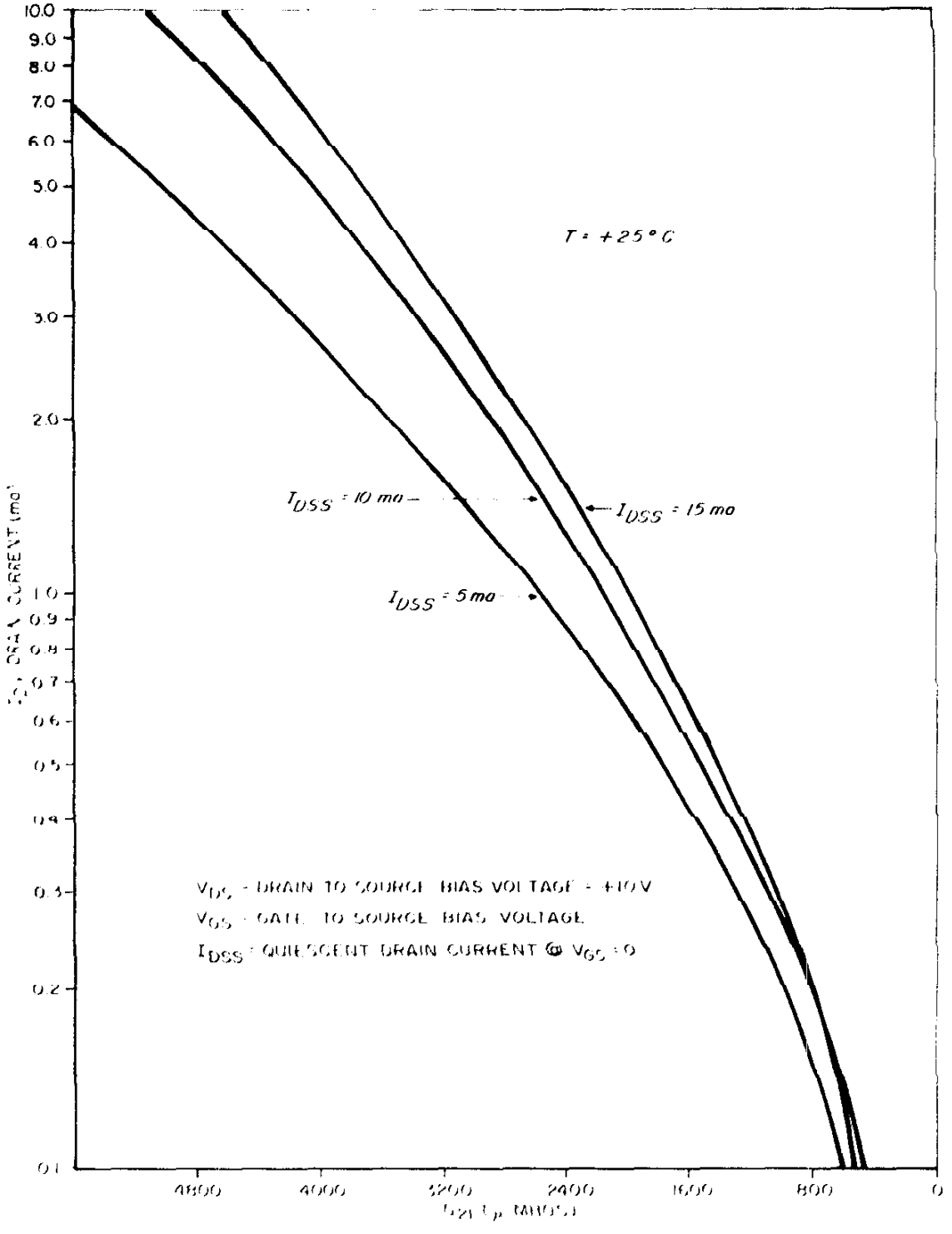

Fig. 20 2N4416 Typical Characteristics

current of approximately 1.82 ma.

Second trial calculation: Assume operation at I_D = 1.8 ma. From the figure, $G_{21} = G_{11}$ = 2900 micro-mhos (less 40% ≈ 1700 micro-mhos). Thus $n_{2_{max}}$ = 6.05 (less 30% ≈ 4.2), and $V_{pd} = \frac{15}{4.2}$ = 3.57 volts. $G_{dl} = 2\, n_2^2\, G_u$ = 381 micro-mhos. Finally, I_{pd} = (3.57) (381) = 1.36 ma.

Final calculation:

I_D	≈	1.4 ma
$G_{21} = G_{11}$	≈	1600 micro-mhos
n_2	≈	4.0
V_{pd}	≈	3.7 volts (2.6 volts RMS)
I_{pd}	≈	1.3 ma
n_1	≈	$\sqrt{\frac{1600 - 120}{11}}$ = 11.6
V_{ps}	≈	1.3 volts (0.92 volts RMS)

Since n_2 was decreased from the maximum value to assure sustained oscillation under worst-case conditions and n_1 was maintained at the optimum value, these values for n_1 and n_2 are not precisely consistent, even for the worst-case conditions assumed. At the high end of the band or for particular transistors which have a higher value of G_{21}, the conditions for sustained oscillation are well surpassed for these values of n_1 and n_2. In an operating circuit, however, the exact relationship, $G_{21} \equiv n_1\, n_2\, G_L$, must be maintained

since it is observed that the output is constant, neither decreasing or increasing. What actually happens is that the transistor operating point shifts into a non-linear region (Class B or C) and conducts over only a portion of a cycle. Under such operation, the quiescent transistor parameters, G_{11}, G_{21}, and G_{22} are reduced by a factor β as shown[14] in Figure 21 until they reach the exact value required for sustained operation. For a given n_1, n_2, and G_u therefore, the conduction angle automatically adjusts to the proper value and the transistor effective parameters assume the new values; $G'_{11} = G'_{21} = \frac{G_{11}}{\beta} = \frac{G_{21}}{\beta}$, $G'_{22} = \frac{G_{22}}{\beta}$. The condition for sustained oscillation is

$$G'_{21} = n_1 n_2 G'_L \quad \text{or}$$

$$\frac{G_{21}}{\beta} = n_1 n_2 \left(G_u + \frac{G_{11}}{\beta n_1^2} + \frac{G_{22}}{\beta n_2^2}\right)$$

Solving for β;

$$\beta = \frac{G_{21} - \frac{n_2}{n_1} G_{11} - \frac{n_1}{n_2} G_{22}}{n_1 n_2 G_u}$$

The effective parameters will now be calculated for the breadboard oscillator.

94.7 MHz: $n_1 = 11.6$, $n_2 = 4.0$, $G_{11} = G_{21} = 1600$, $G_{22} = 30$, $G_u = 10.8$;

Therefore:

$$\beta = 1.92 \; (\theta \approx 190°)$$

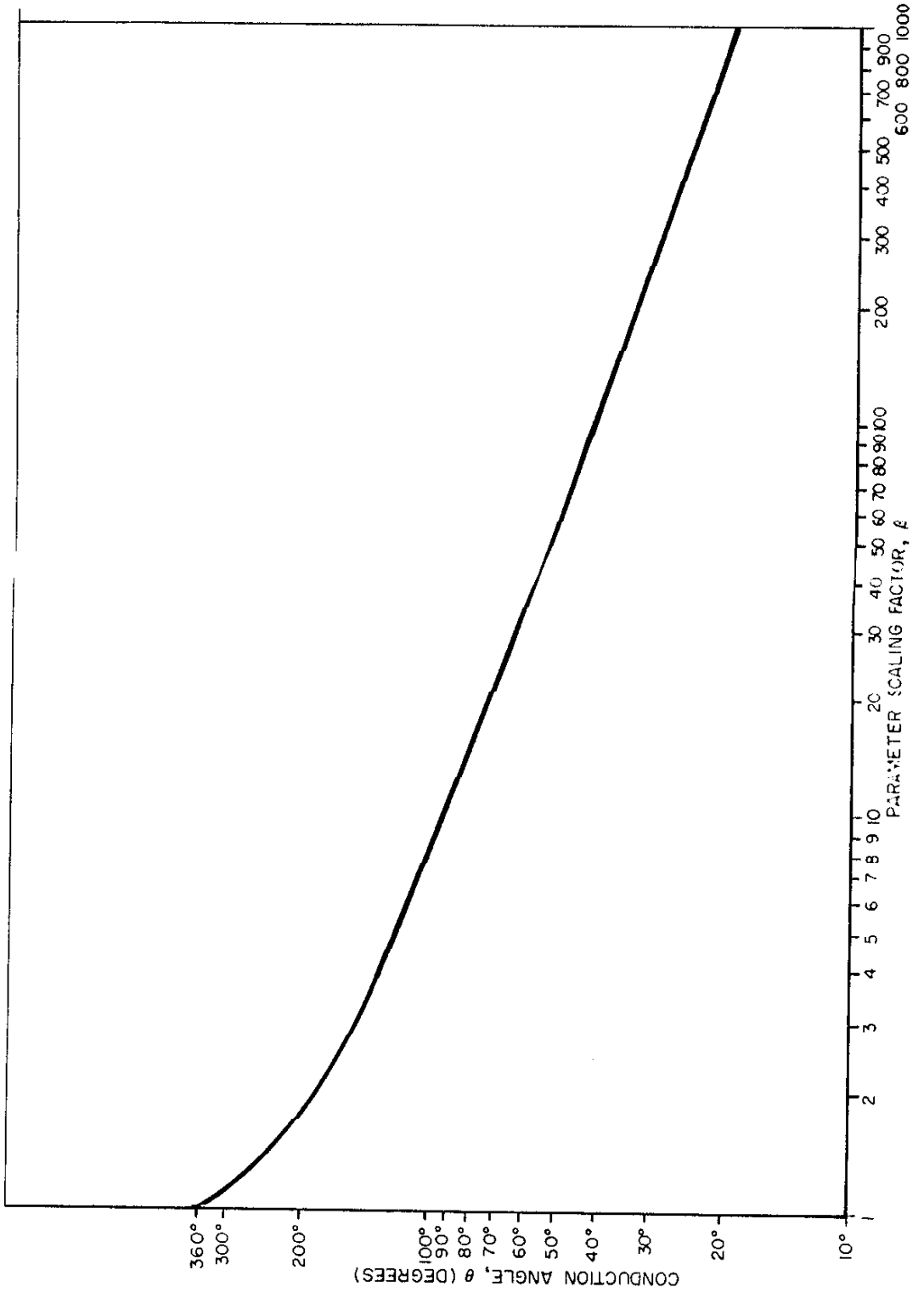

Fig 21 Parameter Scaling Factor vs Conduction Angle

$G'_{11} = G'_{21} = 833$ micro-mhos

$G'_{22} = 15.6$ micro-mhos

122.7 MHz: $n_1 = 11.6$, $n_2 = 4.0$, $G_{11} = G_{21} = 1600$, $G_{22} = 30$, $G_u = 6.4$;

Therefore,

$\beta = 3.24$ ($\Theta \approx 140°$)

$G'_{11} = G'_{21} = 494$ micro-mhos

$G'_{22} = 9.3$ micro-mhos

The oscillator is thus operating approximately in the Class B region. The design value for I_D (d-c drain current) must be modified as shown in Figure 22, such that the fundamental component of the current pulses is the required value to prevent varactor saturation at 94.7 MHz. From the figure, $I_{pd}/I_D \approx 1.50$.

I_{pd} must be re-calculated using the effective transistor parameters since the drain load conductance, G_{dl}, has been changed due to the decrease in G_{11}:

$$G_{dl} = n_2^2 \left(G_u + \frac{G'_{11}}{n_1^2}\right) = 272 \text{ (94.7 MHz)}$$

Thus,

$$I_{pd} = \left(\frac{15}{4.0}\right) (272) = 1.02 \text{ ma, and } I_D = 0.68 \text{ ma.}$$

It remains to calculate the expected value of $S_{\phi}(\omega_m)$. From Equation (35), assuming F = 3 dB:

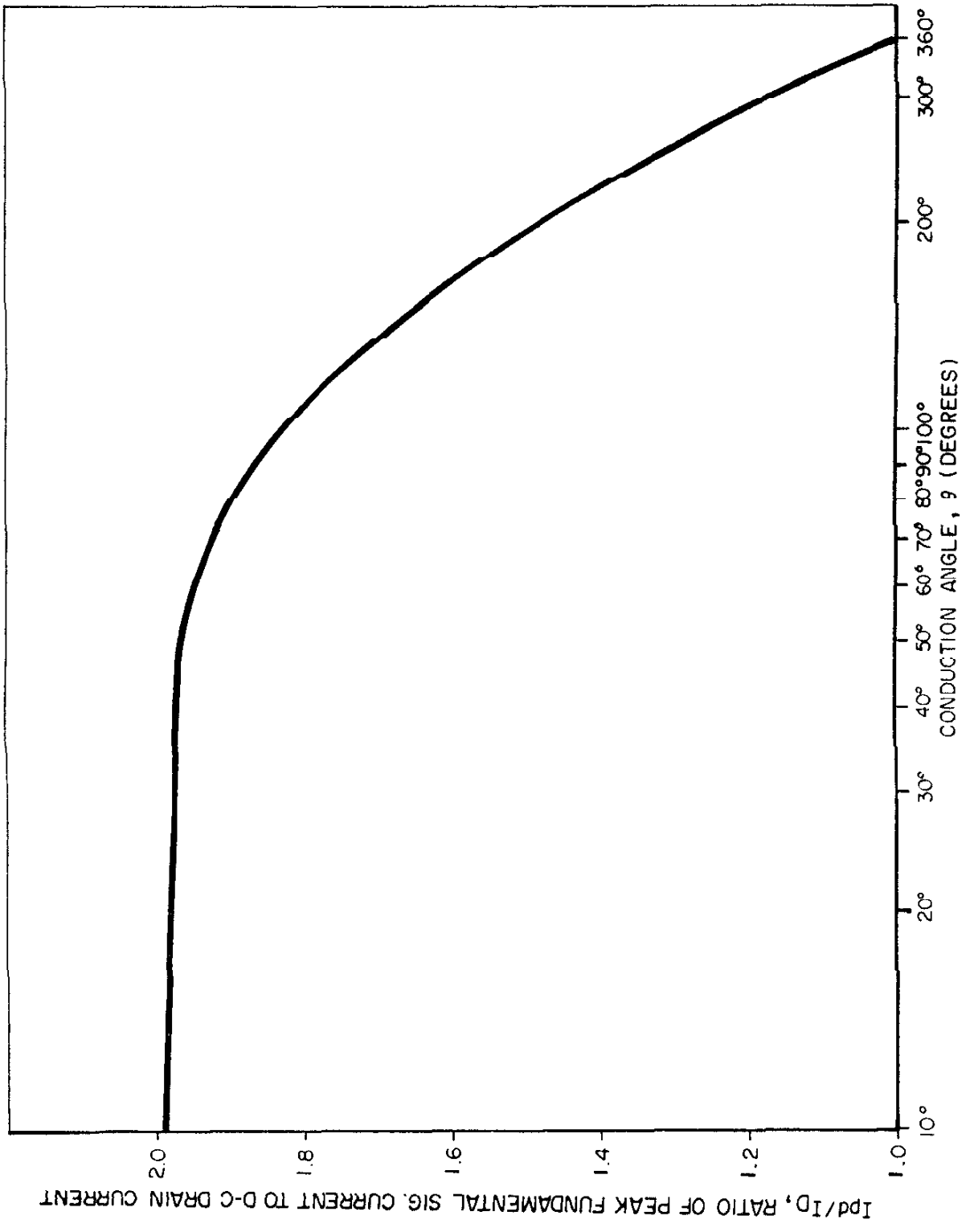

Fig. 22 I_{pd}/I_D vs Conduction Angle

94.7 MHz:

$$G_L = 10.8 + \frac{833}{(11.6)^2} + \frac{15.6}{(4)^2} = 18.0 \text{ micro-mhos}$$

$$Q_L = \frac{L}{2\pi f L G_L} = 146$$

$$P_s = \frac{I^2_{pd}}{2G'_{11}} = \frac{(1.02)^2}{(2)\ (833)} = 625 \text{ microwatts}$$

$$S_\phi \text{ (50kHz)} = -149.5 \text{ dB}$$

122.7 MHz:

$$G_L = 6.4 + \frac{494}{(11.6)^2} + \frac{9.3}{(4)^2} = 10.6 \text{ micro-mhos}$$

$$Q_L = 192$$

$$P_s = \frac{(1.68\ I_D)^2}{2\ G'_{11}} = \frac{(1.14)^2}{(2)\ (494)} = 1.32 \text{ milliwatts}$$

$$S_\phi \text{ (50 kHz)} = -152.5 \text{ dB}$$

A breadboard oscillator was fabricated as per Figure 19 with $n_1 \approx 11.6$, $n_2 \approx 4$, and $I_D \approx 0.7$ ma. The oscillator frequency and power output vs. tuning voltage is shown in Figure 23. The oscillator did not tune the desired frequency range. Calculations indicated an excess stray capacitance of approximately one pf, probably due to wiring capacitance. The excellent temperature characteristic of the oscillator is shown in Figure 24. S_ϕ (50 kHz) is

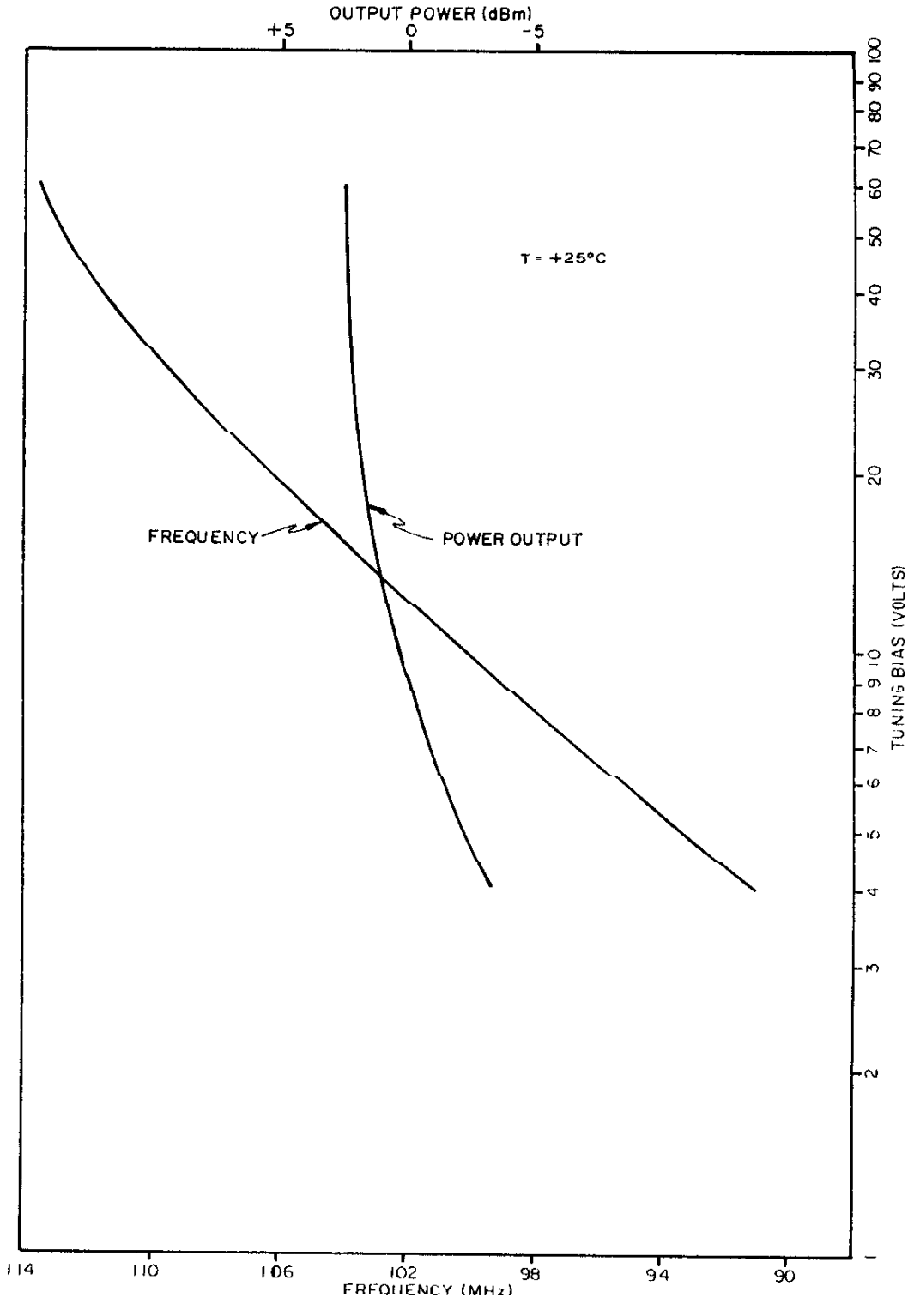

Fig. 23 Frequency and Power Output vs Tuning Bias

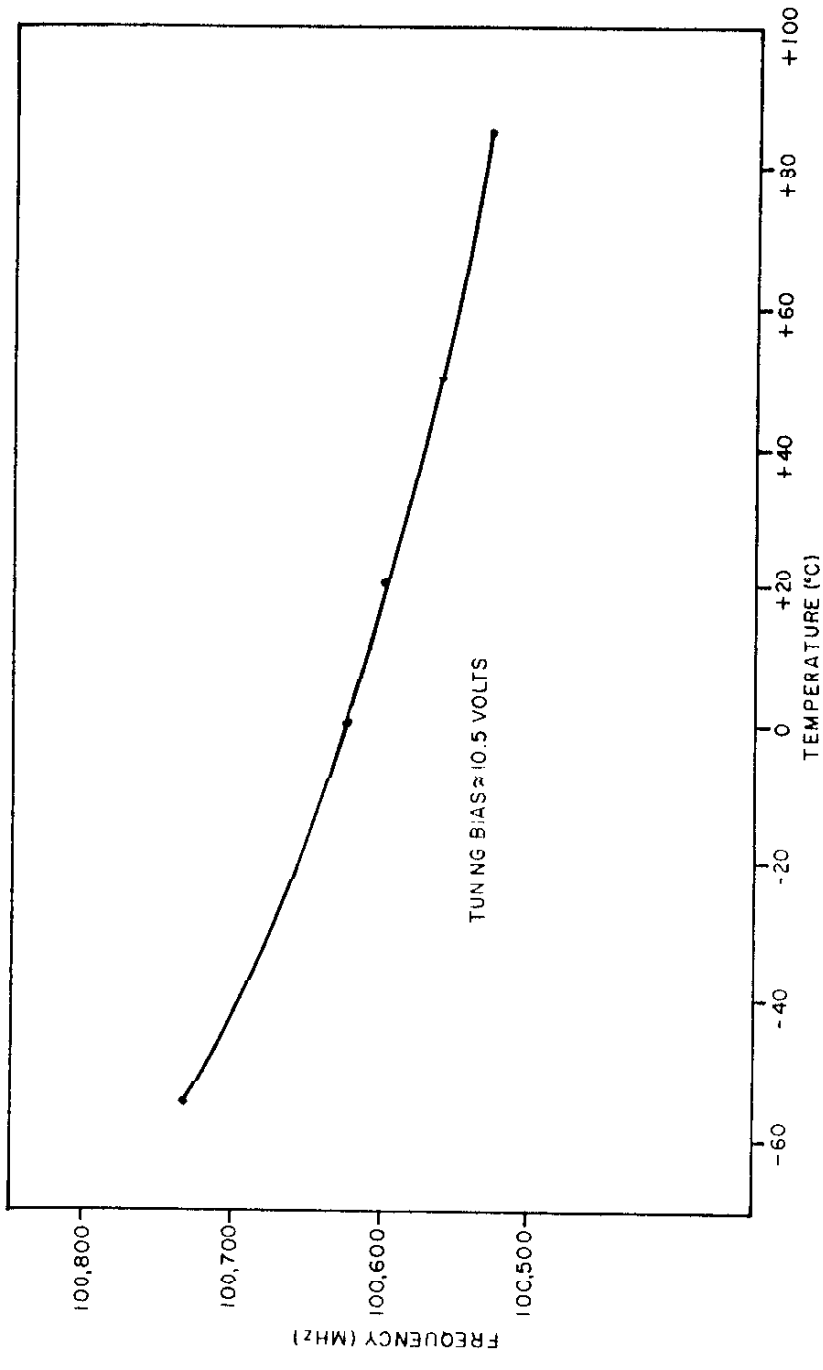

Fig. 24 Frequency vs Temperature

plotted vs. I_D in Figure 25. The optimum value of $S_\phi(\omega_m)$ occurred at approximately 0.9 ma drain current at 5 volts tuning bias. At higher tuning biases, the optimum drain current was correspondingly higher as expected. Figure 26 is a plot of S_ψ (50 kHz) vs tuning voltage and Figure 27 shows the variation of $S_\phi(\omega_m)$ vs ω_m. All measurements were made in a screened room using wet cells for power to avoid extraneous noise sources.

The following conclusions may be drawn from analysis of the breadboard oscillator data:

1) The required frequency range of 94.7 to 122.7 MHz cannot be covered with one oscillator of the present design unless the stray capacitance can be reduced or the noise requirement compromised.

2) $S_\phi(\omega_m)$ cannot be reliably predicted at low tuning voltages. The exact cause of this phenomenon is not known although there are several possible causes:

   a) lowering of the effective Q of the varactors for large signal voltages which swing the varactors close to conduction when the quiescent bias is low.

   b) increased generation of harmonic or sub-harmonic currents at low bias voltages which absorb signal power and thereby lower the *effective Q*.

   c) increased noise due to the increased parametric pumping of the varactors at low bias voltages.

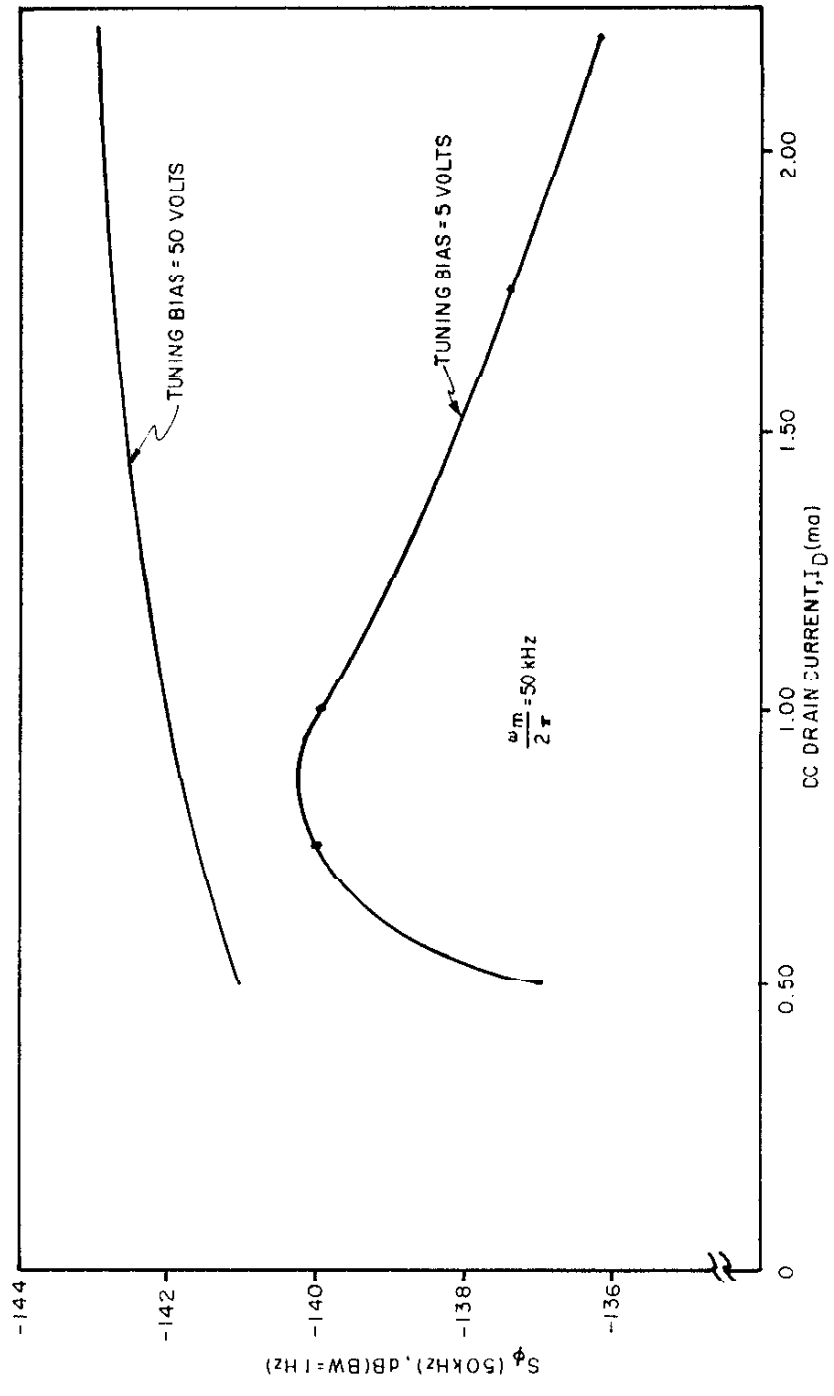

Fig. 15 S_ϕ(50 kHz) vs I_D

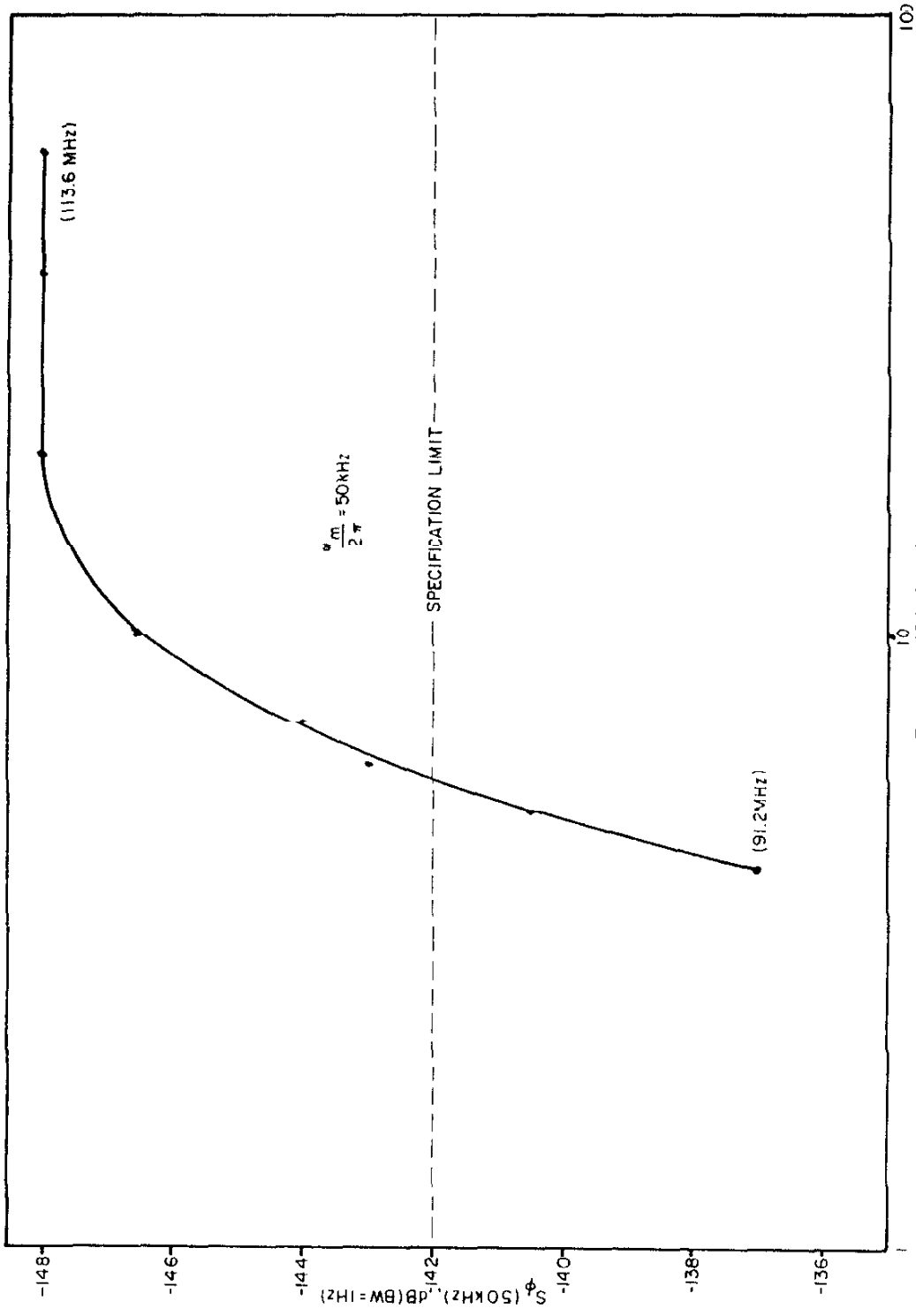

Fig. 26 S_ϕ(50 kHz) vs Tuning Bias

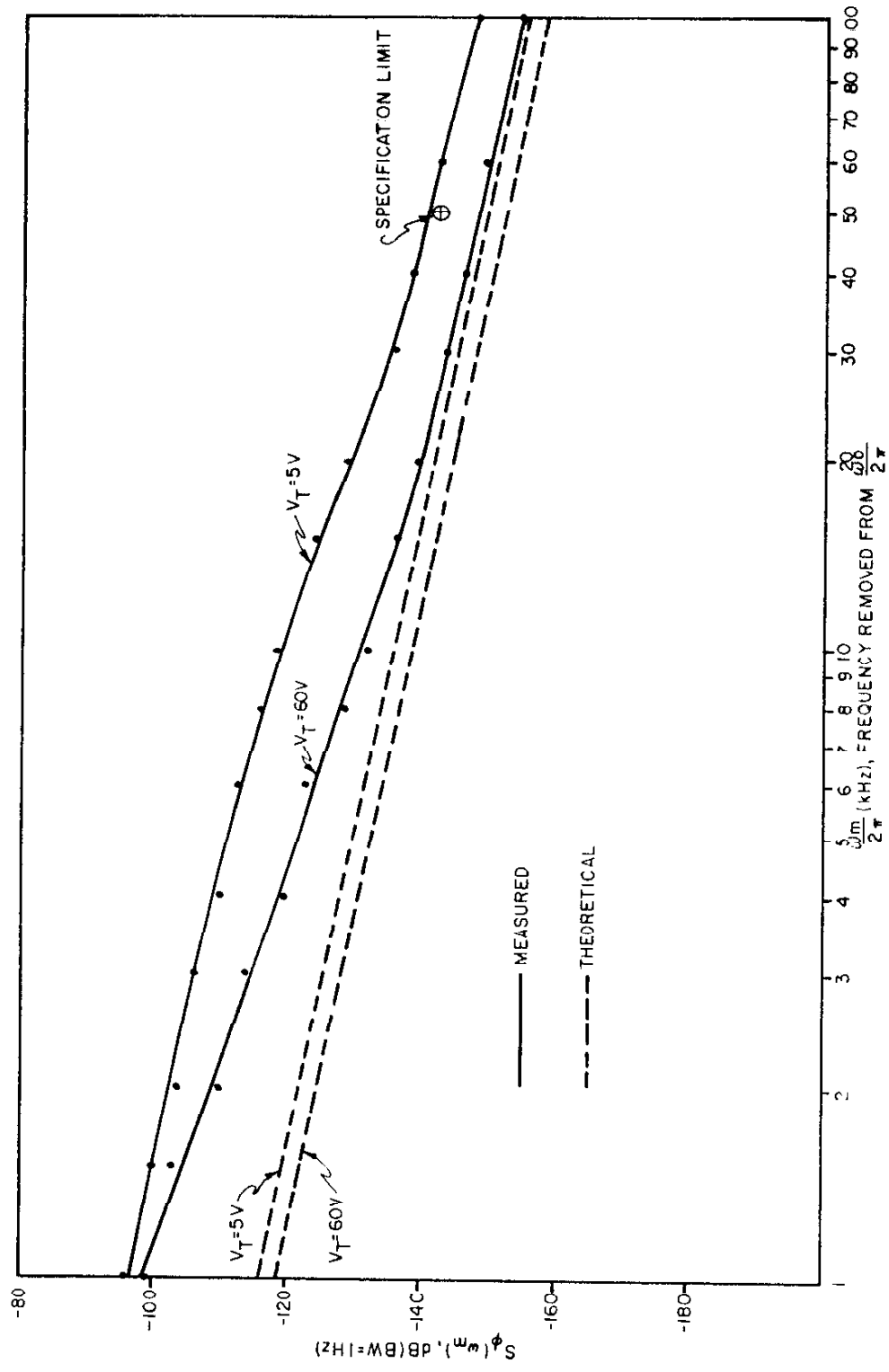

Fig. 27 $S_\phi(\omega_m)$ vs ω_m

Prediction of $S_\phi(\omega_m)$ at higher tuning voltages was fairly accurate at higher values of ω_m, thus confirming the theoretical analysis. Prediction of $S_\phi(\omega_m)$ for low values of ω_m was optimistic because of 1/f noise (neglected in the analysis) which gives rise to an additional 3 dB/octave increase in noise for lower values of ω_m. This results in a 9 dB/octave slope of $S_\phi(\omega_m)$ instead of the predicted 6 dB/octave.

3) The design optimization procedure appears valid. Empirical attempts to improve $S_\phi(\omega_m)$ by shifting turns ratios and drain current indicated that the optimum values were close to the calculated values.

E. Final Design

Because of system interface problems, it was decided to break the frequency range into three bands rather than two, which would otherwise have been satisfactory. The three bands are: 94.7 to 104.7 MHz, 104.7 to 114.7 MHz, and 114.7 to 122.7 MHz. Because of the reduced frequency range of each oscillator, it has not been necessary to use tuning voltages lower than 10 volts. In addition, the reduced frequency range has permitted the addition of a small trimmer capacitor to facilitate reproducibility for volume production. $S_\phi(\omega_m)$ for three prototype oscillators is shown in Figure 28. The specification limit is well exceeded at all frequencies.

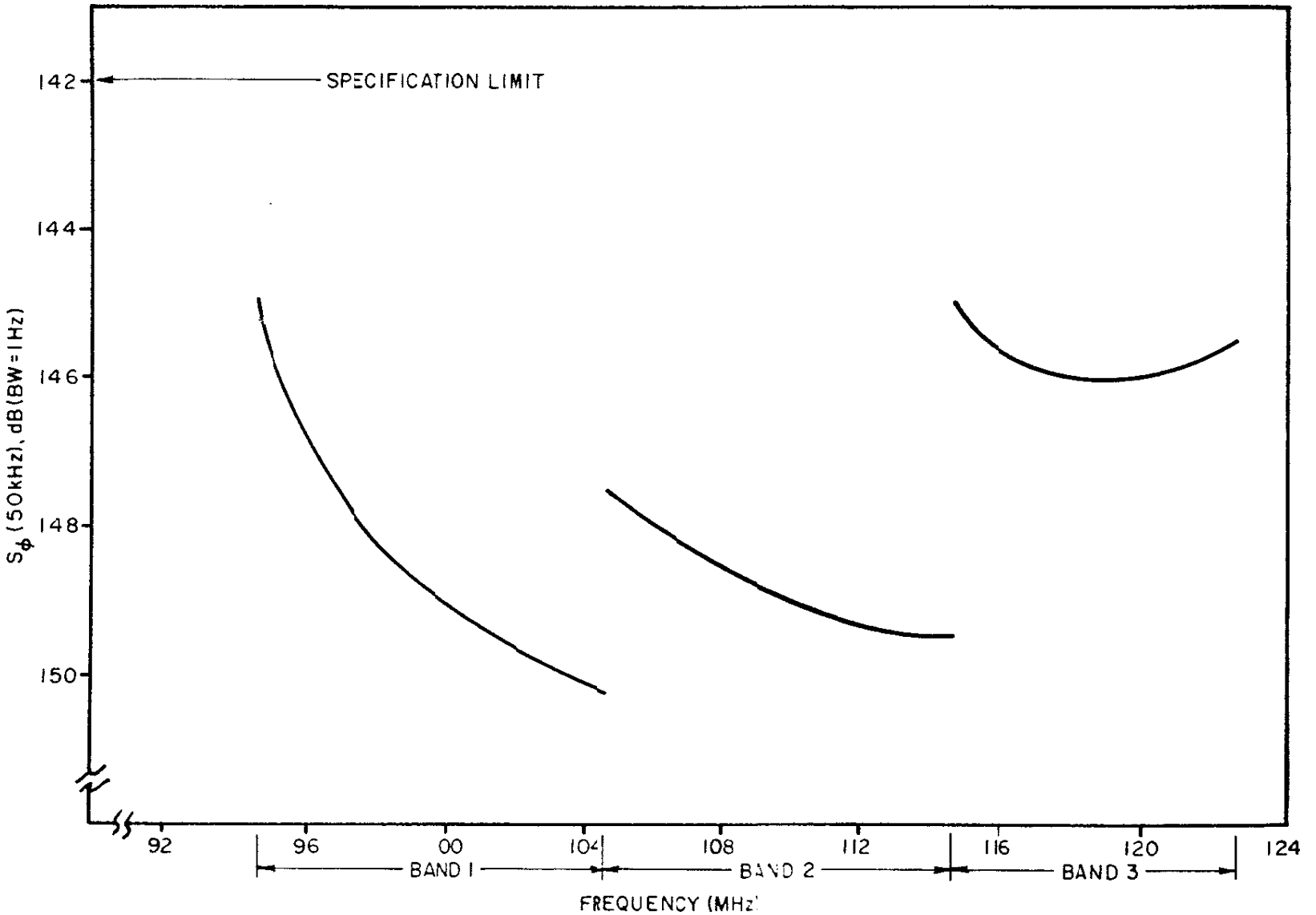

Fig. 28 S_ϕ(50 kHz) vs Frequency for Production Prototype Oscillators

CONCLUSION

The design optimization procedure for varactor tuned oscillators outlined in Section II appears valid when the oscillator power is limited by voltage constraints on the tuning varactors. The extension of the procedure to oscillators limited by other forms of nonlinearity offers an interesting possibility for future work. Entirely different optimum configurations should result depending on whether active device input or output voltages, input or output currents, or input or output power is limited.

The measurement technique outlined in the Appendix has proven to be a most useful apparatus to have available in the laboratory. It has been used for making power spectral density measurements on a variety of oscillators from 1 MHz to 300 MHz. In addition to measuring power spectral density, the technique is also useful for time domain measurements. By applying the output of the auto-correlator to an oscillograph (through an appropriate DC amplifier), a plot of instantaneous frequency vs time is obtained. If, in addition, a simple integrator (such as a single section RC low-pass filter) precedes the oscillograph, a plot of instantaneous phase* vs time is obtained. This provides an excellent, inexpensive method of obtaining long-term or short-term phase and frequency drifts of an oscillator.

---

* The time constant of the integrator must be long compared with the lowest drift components to be measured.

APPENDIX

Measurement Technique

The measurement technique chosen for characterization of oscillator Power Spectral Density (PSD) utilizes the autocorrelation method of Tykulsky[15]. The method is shown in block form in Figure 29.

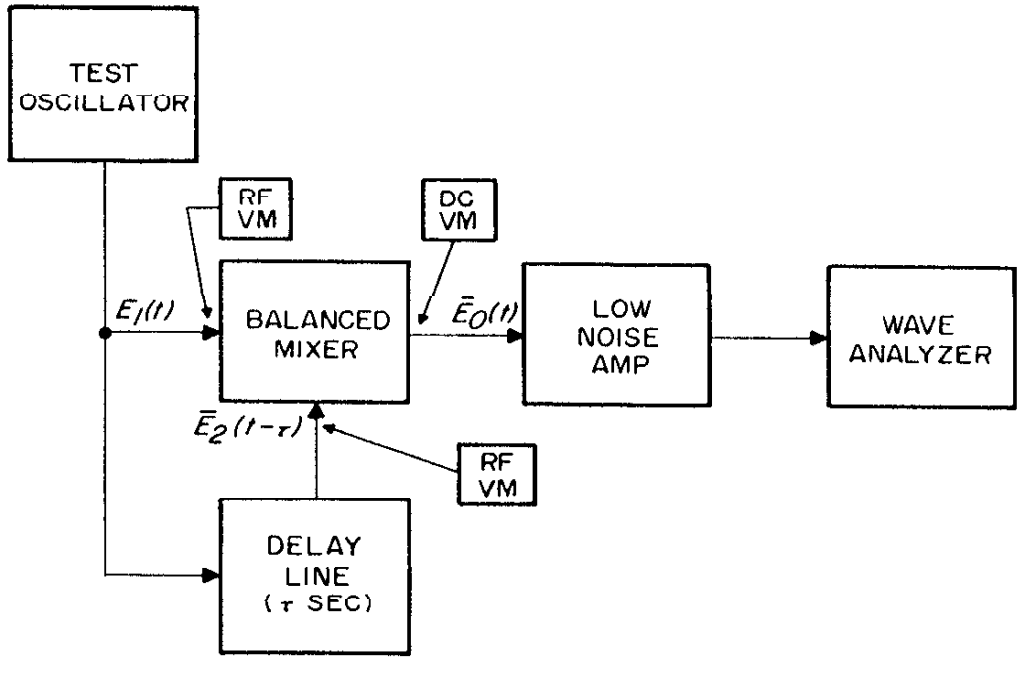

Figure 29

Autocorrelator Block Diagram

The test oscillator is fed directly to one port of a balanced mixer and through a delay (τ seconds) to the other input port. The output of the balanced mixer is

the product of the input signals;

$$\overline{E}_o(t) = k \overline{E}_1(t) \overline{E}_2(t - \tau) \tag{61}$$

where k is the gain constant of the mixer.

For purposes of analysis, assume $\overline{E}_1(t)$ consists of a desired (carrier) signal at ω_o of magnitude E_1, and a random undesired sideband of magnitude E_m removed from ω_o by ω_m as shown in Figure 30.

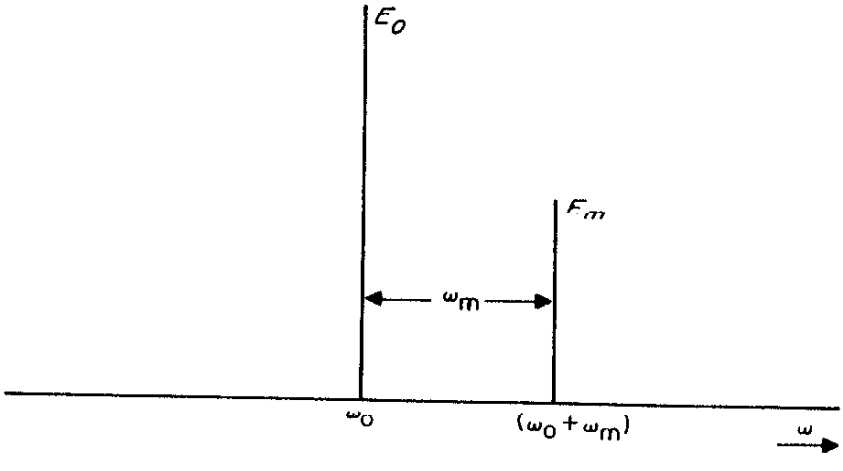

Figure 30

Assumed Input Spectrum

This can be represented[16] by pairs of equal magnitude symmetrical (AM) sidebands and asymmetrical (FM) sidebands as shown in Figure 31.

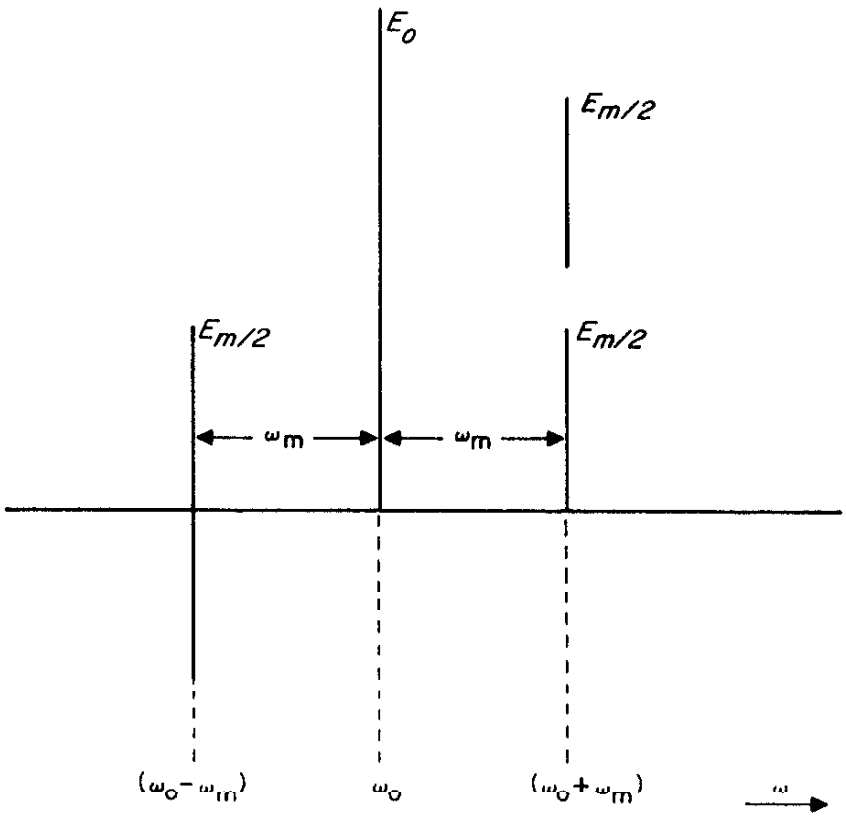

Figure 31

Equivalent Input Spectrum

The output of the mixer will be analyzed for both cases.

1. FM Components:

Assuming small index of modulation ($m < 0.5$) $\overline{E}_1(t)$ may be represented by;

$$\overline{E}_1(t) = E_1 \left[\cos \omega_o t - \frac{m}{2} \cos (\omega_o - \omega_m)t + \frac{m}{2} \cos (\omega_o + \omega_m) t \right] \quad (62)$$

$$\overline{E}_2(t) = E_2\left[\cos\omega_o(t-\tau) - \frac{m}{2}\cos(\omega_o-\omega_m)(t-\tau) + \frac{m}{2}\cos(\omega_o+\omega_m)(t-\tau)\right] \quad (63)$$

Substitution of (62) and (63) into (61) yields (eliminating terms centered on $2\omega_o$);

$$\overline{E}_o(t)_{FM} = \frac{k E_1 E_2}{2}\left[\cos\omega_o\tau\ (1 + \frac{m^2}{2}\cos\omega_m\tau) - 2m\sin\omega_o\tau\ \sin\frac{\omega_m\tau}{2}\cos\omega_m(t-\tau/2) - \frac{m^2}{2}\cos(\omega_o+\omega_m)\tau\cos(2\omega_m t)\right] \quad (64)$$

For $m \ll 1$ (certainly true for noise modulation), (64) reduces to:

$$\overline{E}_o(t)_{FM} = \frac{k E_1 E_2}{2}\left[\cos\omega_o\tau - 2m\sin(\omega_o\tau)\sin(\frac{\omega_m\tau}{2})\cos\omega_m(t-\tau/2)\right] \quad (65)$$

Thus the output consists of a d-c term and a term at ω_m (the desired output). The system has maximum sensitivity to FM when $\sin\omega_o\tau = \pm 1$ (and thus $\cos\omega_o\tau = 0$, hence no d-c output) or;

$$\tau = \frac{(2N+1)}{\omega_o}\frac{\pi}{2} \qquad (N = \text{integer}) \quad (66)$$

This occurs when the ω_o terms in $\overline{E}_1(t)$ and $\overline{E}_2(t-\tau)$ are in phase quadrature and the delay line is an integral number of odd quarter-wavelengths at ω_o.

For τ as specified in (66), (65) reduces to;

$$\overline{E}_o(t)_{FM} = -k E_1 E_2 m \sin(\frac{\omega_m\tau}{2})\cos\omega_m(t-\tau/2) \quad (67)$$

Note that:

$$E_{o_{FM}} \propto \sin \frac{\omega_m \tau}{2} \tag{68}$$

Equation (68) is in contradiction to Tykulsky's equation (1) which holds that E_o should be proportional to $\sin \omega_m \tau$. The correctness of (68) has been established by measurement as will be shown later. From (68) it is apparent that the system has maximum sensitivity when $\sin \left(\frac{\omega_m \tau}{2} \right) = \pm 1$, or;

$$\tau_{OPT} = \frac{(2M + 1)}{\omega_m} \pi \qquad (M = \text{integer}) \tag{69}$$

This occurs when the delay line is an integral number of odd half-wavelengths at ω_m.

2. AM Components:

For the AM case, $\overline{E}_1(t)$ may be represented by;

$$\overline{E}_1(t) = E_1 \left[\cos \omega_o t + \frac{m}{2} \cos (\omega_o - \omega_m) t + \frac{m}{2} \cos (\omega_o + \omega_m) t \right] \tag{70}$$

and $\overline{E}_2 (t - \tau)$ then becomes;

$$\overline{E}_2(t-\tau) = E_2 \left[\cos \omega_o (t-\tau) + \frac{m}{2} \cos (\omega_o - \omega_m)(t-\tau) + \frac{m}{2} \cos (\omega_o + \omega_m)(t-\tau) \right] \tag{71}$$

Substitution of (70) and (71) into (61) yields (eliminating terms centered on $2 \omega_o$, and again assuming $m \ll 1$);

$$\bar{E}_o(t)_{AM} = \frac{k E_1 K_2}{2} \left[\cos \omega_o \tau + 2m \cos (\omega_o \tau) \cos \left(\frac{\omega_m \tau}{2} \right) \cos \omega_m (t - \tau/2) \right] \quad (72)$$

As with the FM case, the output consists of a d-c term and a term at ω_m. The system has maximum sensitivity to AM when $\cos \omega_o \tau = 1$ (and hence maximum d-c output), or;

$$\tau = \frac{P}{\omega_o} \pi \qquad (P = \text{integer}) \quad (73)$$

This occurs when the ω_o terms in $\bar{E}_1(t)$ and $\bar{E}_2(t-\tau)$ are in phase or 180° out of phase and the delay line is an integral number of even half-wavelengths (including $\tau = 0$) at ω_o. For τ as specified in (73), (72) reduces to;

$$\bar{E}_o(t)_{AM} = \frac{k E_1 E_2}{2} + k E_1 E_2 m \cos \left(\frac{\omega_m \tau}{2} \right) \cos \omega_m (t - \tau/2) \quad (74)$$

The maximum output at ω_m occurs when $\cos \left(\frac{\omega_m \tau}{2} \right) = 1$, or;

$$\tau_{OPT} = \frac{Q}{\omega_m} \pi \qquad (Q = \text{integer}) \quad (75)$$

This occurs when the delay line is an integral number of even half-wavelengths (including $\tau = 0$) at ω_m.

Thus the measurement system is capable of determining sideband levels directly and separating them into AM and FM components. In a practical situation the sensitivity of the system is determined by several factors:

1) It is desirable to make E_1 and E_2 as large as possible. However, practical mixers have only a limited dynamic range for linear operation such that (61) remains valid. This establishes an upper bound on E_o.

2) The lower bound on E_o depends on noise originating in the mixer and amplifier. An amplifier with a low noise figure is essential.

3) It is often necessary to compromise from the optimum value of τ given by (69) due to size and/or insertion loss constraints.

A measurement system was constructed in the laboratory using the following equipment:

1) Mixer — A Hewlett-Packard Model 10514A balanced mixer was chosen because of its wide bandwidth (0.2 to 500 MHz), low conversion loss and excellent dynamic range. A schematic of the mixer is shown in Figure 32. D_1 through D_4 are hot-carrier diodes with matched V-I characteristics. The "L" and "R" ports use broadband transformers matched to 50 ohms (nominal) and were used as the input ports for $\bar{E}_1(t)$ and $\bar{E}_2(t-\tau)$ respectively. Output was taken from the direct-coupled "X" port. Optimum performance was obtained with input powers of 10 to 40 mW and 1 to 2 mW respectively. Dynamic range is lowered with less input power and excessive nonlinearity results from higher input powers.

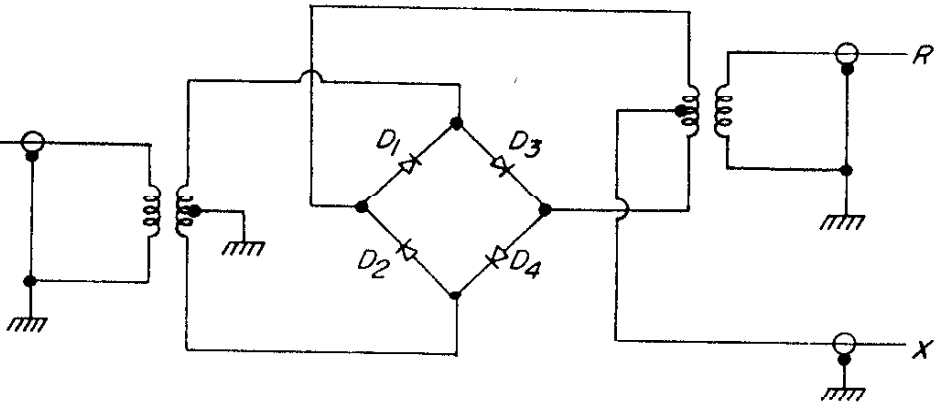

Figure 32
Balanced Mixer

2) Delay Line — 50 ohm transmission line was used as the delay line in order to provide as wide a bandwidth as possible to enable PSD measurements over a wide range of oscillator frequencies. Since the difference in optimum power levels between the "L" and "R" mixer ports is approximately 10 dB, the transmission line should not have more loss than this to avoid the need for amplification. 1000 feet of 1/2 inch, 50 ohm, foamed dielectric cable (Phelps-Dodge FX-50 "Foam-Flex") proved quite satisfactory. This cable has 8.5 dB insertion loss at 100 MHz and provides a τ of 1.32 microseconds.

3) Low Noise Amplifier — A Radiation Electronics Model R-201 amplifier was used to provide 80 dB of gain (flat from 500 Hz to 75 kHz) with a noise figure of less than 2 dB. The amplifier was preceded with a

simple low pass filter to prevent saturation of the input stages by the carrier and second harmonic components at the mixer output. Measurements above 50 kHz are made with no amplifier or with a suitable higher frequency amplifier.

4) Wave Analyzer — A Hewlett-Packard Model 310-A Wave Analyzer provides PSD measurements from 1 kHz to 1.5 MHz with bandwidths of 0.2, 1.0, and 3.0 kHz.

5) Ancillary Items — Two Boonton Electronic Model 91-CA RF Voltmeters were used to continuously monitor the voltages at the mixer input ports and a Hewlett-Packard Model 410-B VTVM was used to monitor the d-c output of the mixer to determine the relative phase of the input signals.

Calibration of the equipment is quite simple and is carried out as follows:

a) FM Sidebands — A test oscillator at ω_o capable of being frequency modulated is connected to the input. τ or ω_0 is adjusted slightly to satisfy (66) and thus validate (67). The correct condition is obtained when the mixer d-c output is zero. The test oscillator is then deviated at ω_m to produce a known sideband level at $\omega_0 \pm \omega_m$ (measureable with an r-f spectrum analyzer). For small index of modulation ($m < 0.5$), $\bar{E}_o(t)_{FM}$ is linearly proportional to m. Thus

calibration may be performed with easily observable sideband levels (say 40 dB) and then $\bar{E}_o(t)_{FM}$ linearly extrapolated down to the mixer noise level.

b) AM Sidebands — Calibration for AM sidebands is accomplished in a manner analogous to that for FM. τ is reduced to zero (the delay line is replaced by an appropriate attenuator). Under this condition the d-c output should be at a maximum value, thus satisfying (73) and validating (74). The test oscillator is then amplitude modulated at ω_m to produce a known sideband level, whence the relationship (gain constant) between $\bar{E}_o(t)_{AM}$ and sideband level is uniquely determined.

Using the equipment and calibration procedure above, the calibration curves of Figure 33 were obtained. The AM curve is valid for any modulating frequency, ω_m. The FM curve is plotted for $\frac{\omega_m}{2\pi} = 10$ kHz. For $\frac{\omega_m}{2\pi} < 10$ kHz, $\sin\left(\frac{\omega_m \tau}{2}\right) \approx \left(\frac{\omega_m \tau}{2}\right)$, and (67) reduces to,

$$\bar{E}_o(t)_{FM} = -k E_1 E_2 m \omega_m \tau/2 \cos \omega_m (t-\tau/2) \tag{76}$$

and thus,

$$\bar{E}_o(t)_{FM} \propto \omega_m \qquad \left(\frac{\omega_m}{2\pi} < 10 \text{ kHz}\right) \tag{77}$$

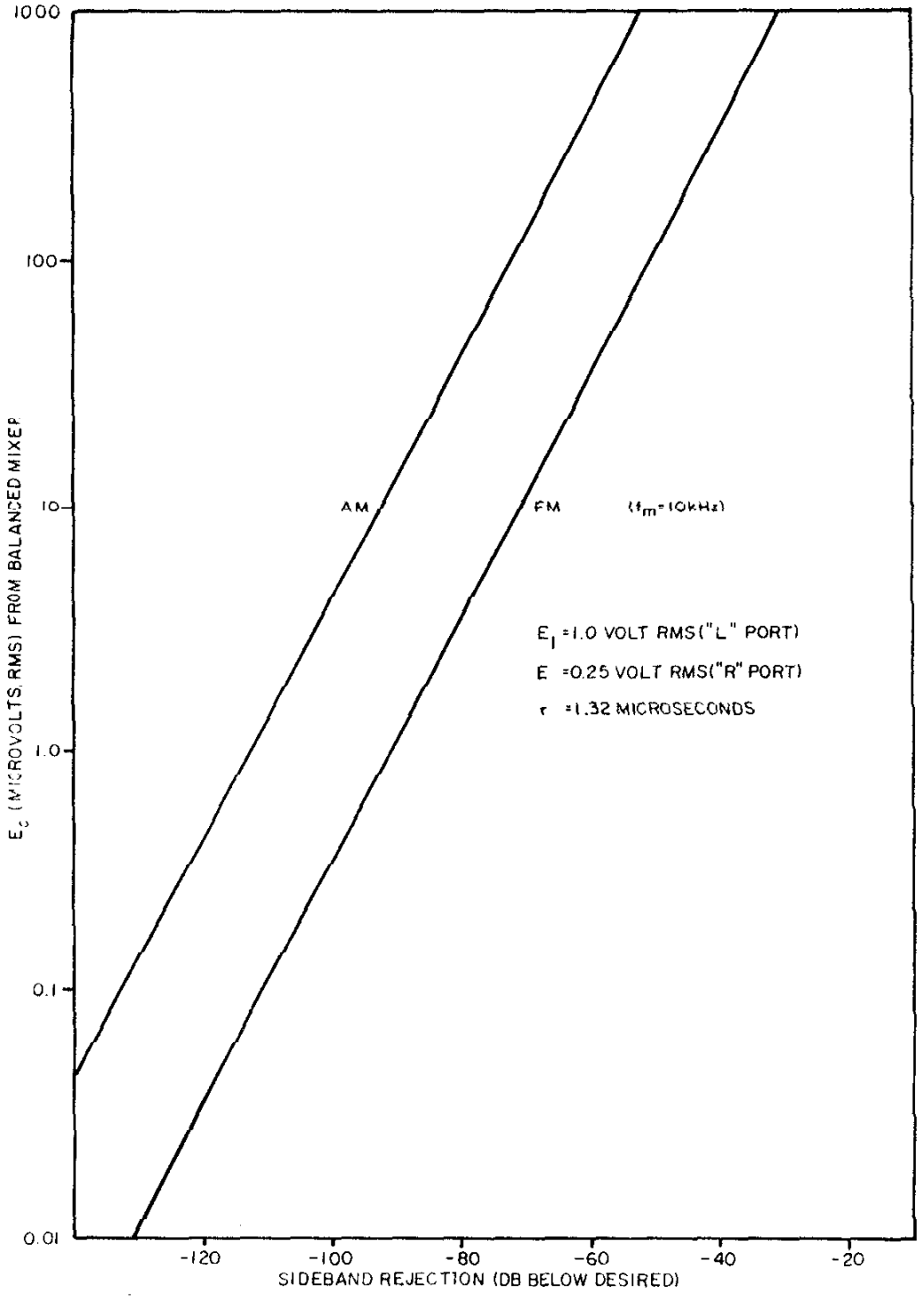

Fig. 33 Calibration Curves

Hence for $\frac{\omega_m}{2\pi} < 10$ kHz, the sensitivity of the measurement system decreases at a rate of 6 dB/octave.

Figure 34 provides FM correction factors for $\frac{\omega_m}{2\pi} > 10$ kHz.

The noise floor for $\bar{E}_o(t)_{FM}$ in Figure 33 is a function of measurement bandwidth.

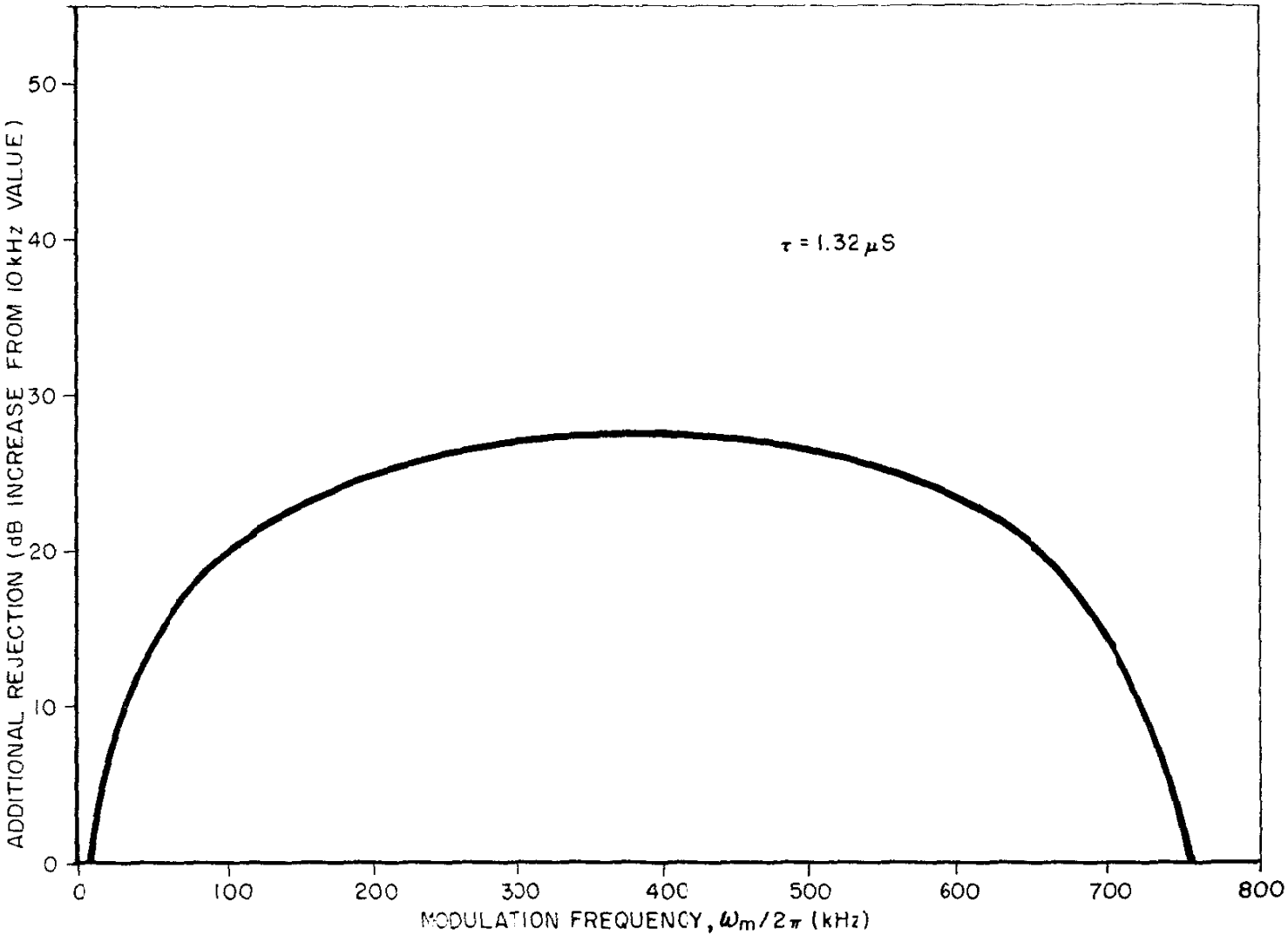

Fig. 34 FM Correction Curve for $\frac{\omega_m}{2\pi} > 10$ kHz

BIBLIOGRAPHY

1. L. S. Cutler & C. L. Searle, "Some Aspects of the Theory and Measurement of Frequency Fluctuations in Frequency Standards", Proc. IEEE, v 54, pp 136-154, Feb., 1966.

2. W. B. Davenport & W. L. Root, "Random Signals and Noise", Sec 8.5, p 158 ff; New York, McGraw-Hill; 1958

3. Davenport & Root, op. cit., Chapter 6

4. W. A. Edson, Vacuum-Tube Oscillators; New York; Wiley; 1953

5. W. A. Edson, "Noise in Oscillators", Proc. IRE, v 48, pp 1454-1466, August, 1960

6. E. Hafner, "The Effects of Noise in Oscillators", Proc. IEEE, v 54, pp 179-198, Feb., 1966

7. D. B. Leeson, "A Simple Model of Feedback Oscillator Noise Spectrum", Proc. IEEE, v 54, pp 329-330, Feb., 1966

8. J. A. Mullen, Background Noise in Nonlinear Oscillators", Proc. IEEE, v 48, pp 1467-1472, Aug., 1960

9. L. R. Malling, "Phase-Stable Oscillators for Space Communications, Including the Relationship Between the Phase Noise, the Spectrum, the Short-term Stability, and the Q of the Oscillator", Proc. IRE, pp 1656-1664, July, 1962

10. Hafner, op. cit., p 179

11. Leeson, op. cit.

12. W. W. Macalpine & R. O. Schildknecht, "Coaxial Resonators With Helical Inner Conductor", Proc. IRE, v 47, pp 2099-2105, Dec., 1959

14. Edson, op. cit., p 161

15. A. Tykulsky, "Spectral Measurements of Oscillators", Proc. IEEE, v 54, p. 306, Feb., 1956

16. S. Goldman, Frequency Analysis, Modulation and Noise, New York: McGraw-Hill; 1948; Chap. 5